NACA TN 2558 8943

TECH LIBRARY KAFB, NM
0065567

NATIONAL ADVISORY COMMITTEE FOR AERONAUTICS

TECHNICAL NOTE 2558

SOME EFFECTS OF VARIATIONS IN SEVERAL PARAMETERS INCLUDING FLUID DENSITY ON THE FLUTTER SPEED OF LIGHT UNIFORM CANTILEVER WINGS

By Donald S. Woolston and George E. Castile

Langley Aeronautical Laboratory
Langley Field, Va.

Washington
December 1951

AFMDC
TECHNICAL
AFL

TECH LIBRARY KAFB, NM
0065567

NATIONAL ADVISORY COMMITTEE FOR AERONAUTICS

NACA TN 2558

SOME EFFECTS OF VARIATIONS IN SEVERAL PARAMETERS INCLUDING FLUID DENSITY ON THE FLUTTER SPEED OF LIGHT UNIFORM CANTILEVER WINGS

By Donald S. Woolston and George E. Castile

SUMMARY

An experimental investigation has been made of some effects of variations in several parameters, including fluid density, on the flutter characteristics of light uniform cantilever wings. The assortment of wings tested covered a variety of positions of the elastic axis and center of gravity and values of the aspect ratio of 8, 6, and 4. The relative-density parameter $1/\sqrt{\kappa}$ (where κ is representative of the ratio of fluid density to wing mass) was varied over a range of values from 1.2 to nearly 14. Special emphasis has been placed on the lower values.

The experimental investigation has been supplemented by an analytical investigation based on the two-dimensional aerodynamic theory for incompressible flow. In a few instances corrections for the effects of finite span have been made. In general, the theoretical results followed the trends indicated by experiment except at very low values of the relative-density parameter $\left(1/\sqrt{\kappa}\right.$ less than $3)$. For these low values the analytical considerations employed indicated a freedom from flutter not found experimentally. At higher values of $1/\sqrt{\kappa}$ the flutter-speed coefficient is shown to decrease with decreasing values of $1/\sqrt{\kappa}$ and to be nearly proportional to the inverse of the square root of the air density.

INTRODUCTION

The trend toward flight of airplanes at high speeds and high altitudes has given increased significance to the problem of the effects of Mach number and variations in density on wing flutter characteristics. Experimental and theoretical investigations of the problem have been made, for example, in references 1 and 2. The present investigation is intended to make further contributions to the subject.

In reference 1 the results of an experimental investigation of the effects of variations in fluid density are presented. The flutter data are shown as a function of a relative-density parameter $1/\sqrt{\kappa}$, where κ is the ratio of the mass of a cylinder of the surrounding fluid with diameter equal to the chord of the wing to the mass of the wing. Two fairly heavy wings (with values of $1/\sqrt{\kappa}$ greater than 9) were tested over a range of Mach numbers and density. After some simple modifications for the effects of compressibility and wave length, the dynamic pressure at flutter was shown to be nearly constant over the full range of densities tested.

A part of the work presented in reference 2 deals with the theoretical effects of variations in density. Considerably lighter wings (values of $1/\sqrt{\kappa}$ from 3 to 5) than those treated in reference 1 were included in the study. At the higher values of the relative-density parameter the nearly constant dynamic pressure at flutter noted in reference 1 was indicated. As this density parameter was decreased to values typical of very light wings, an abrupt change occurred in the behavior of the flutter curves. Since the wings tested in reference 1 were not sufficiently light to lie in this critical range, and since some light airplanes, or components of heavier airplanes, at low altitudes may approach this range, a further experimental investigation seemed desirable.

One of the purposes of the present paper is to extend the experimental study of the effects of density variations to low values of the relative-density parameter and thus to extend the work of reference 1. Furthermore, a wider assortment of wings, giving a broader range of structural parameters, is studied than was treated in reference 1. This assortment of wings covers a variety of positions of the elastic axis and center of gravity, a range of values of the ratio of bending frequency to torsional frequency, and values of the aspect ratio of 8, 6, and 4. The experiments were conducted in different mixtures of air and Freon-12, which resulted in density variations equivalent to variations in altitude from sea level to approximately 40,000 feet. For each case of experimental flutter, a theoretical calculation for the corresponding conditions at flutter was undertaken. In this work use was made of an analysis of the Rayleigh type in which two-dimensional, incompressible aerodynamic coefficients were employed. In a few selected cases corrections for finite span have been applied by the method of reference 3. The analytical treatment as given herein is not complete and should be extended, with particular emphasis on the low values of the relative-density parameter appropriate to light airplanes.

SYMBOLS

a	nondimensional distance of elastic axis from midchord measured in half-chords, positive for positions of elastic axis behind midchord
A	aspect ratio
b	wing half-chord, feet
c	wing chord, feet
EI	bending stiffness of wing
g	structural damping coefficient considered as variable in solution of flutter determinant
GJ	torsional stiffness of wing
I_α	mass moment of inertia per unit length referred to wing elastic axis
l	semispan of wing, feet
L_h	aerodynamic wing-lift coefficient due to bending oscillation of the wing
L_α	aerodynamic wing-moment coefficient due to torsional oscillations of the wing about its quarter chord
M_h	aerodynamic moment coefficient about wing quarter-chord point due to bending oscillations of the wing
M_α	aerodynamic moment coefficient about wing quarter-chord point due to torsional oscillations of wing about its quarter chord
m	mass per unit length
M	Mach number
q	dynamic pressure, pounds per square foot
r_α	nondimensional radius of gyration relative to elastic axis $\left(\sqrt{I_\alpha/mb^2}\right)$

S_α static moment per unit length referred to wing elastic axis, positive for center of gravity behind elastic axis

v flutter speed, feet per second

x_α nondimensional distance of center of gravity from elastic axis measured in half-chords, positive for positions of center of gravity behind elastic axis

κ relative-density parameter $\left(\pi\rho b^2/m\right)$

ρ density of testing medium, slugs per cubic foot

ω angular frequency at flutter, radians per second

ω_{h_1} angular frequency of first uncoupled bending mode, radians per second

ω_{h_2} angular frequency of second uncoupled bending mode, radians per second

ω_α angular frequency of first uncoupled torsional mode, radians per second

APPARATUS AND TESTS

Models

Semispan models of balsa rib and skin construction supported by a single spar were used in this investigation and were designed to give a low wing density. The models were slotted chordwise into 2-inch sections in order to avoid possible unknown changes in stiffness inherent in complicated glued structures. (See fig. 1.)

Three positions of the elastic axis were obtained by placing the spar 20, 30, and 40 percent of the chord behind the leading edge. The chord of all models was kept constant (1 ft.), whereas the semispan was varied to provide aspect ratios of 8, 6, and 4. The properties of the models are presented in table I. Models are designated by three numbers separated by dashes: the first two give, respectively, the approximate locations of the elastic axis and of the center of gravity in percent chord from the leading edge, and the third specifies the ratio of the wing semispan to the chord. The frequencies given in the table are

uncoupled frequencies and were calculated from the measured stiffness, mass, and moment of inertia of the wing. Moment of inertia was measured by swinging a section of the wing as a torsional pendulum in a partial vacuum of two inches of mercury.

Testing Techniques

The models were mounted as cantilevers in the Langley 4.5-foot flutter research tunnel described in reference 1. The flutter tests were conducted with different mixtures of air and Freon-12 to provide variations in density. The airspeed in the tunnel was increased gradually until flutter was observed. The airspeed was then reduced immediately to prevent destruction of the model. At the point of flutter an oscillograph record of the model frequencies was taken and the tunnel temperature, tunnel pressure, and dynamic pressure were recorded. Where Freon-12 was employed, the percentage of Freon-12 in the testing medium was obtained after each test.

Wherever possible models were tested over the full density range of the tunnel; that is, at pressures from 30 inches of mercury in Freon-12 to 4 inches of mercury in air. These pressures correspond to a range of altitudes from sea level to approximately 40,000 feet and provide values of $1/\sqrt{\kappa}$ from 1.2 to about 14.

ANALYSIS

In the theoretical determination of the flutter characteristics of the cases considered in this investigation, application has been made of an analysis of the Rayleigh type, based on uncoupled modes and two-dimensional incompressible air-force coefficients. In all cases the first three uncoupled modes of the system (namely first bending, first torsional, and second bending) have been considered. The determinantal equation of the flutter condition in these three degrees of freedom, derived from the Lagrangian equations of equilibrium, may be expressed as (see, for example, reference 4, chapter IX):

$$\begin{vmatrix} A_{11}\left[1 - \omega_{h_1}{}^2\Omega\right] + C_{11} & A_{12} + C_{12} & A_{13} + C_{13} \\ A_{21} + C_{21} & A_{22}\left[1 - \omega_{h_2}{}^2\Omega\right] + C_{22} & A_{23} + C_{23} \\ A_{31} + C_{31} & A_{32} + C_{32} & A_{33}\left[1 - \omega_{\alpha}{}^2\Omega\right] + C_{33} \end{vmatrix} = 0 \quad (1)$$

where the A and C coefficients are constants computed from the inertial properties of the system, the uncoupled modes, and the appropriate aerodynamic coefficients. They are given by:

$$
\begin{aligned}
A_{11} &= \int_0^l m\left[f_{h_1}(x)\right]^2 dx & C_{11} &= \pi\rho \int_0^l b^2\alpha\left[f_{h_1}(x)\right]^2 dx \\
A_{12} = A_{21} &= \int_0^l m f_{h_1}(x) f_{h_2}(x)\,dx = 0 & C_{12} = C_{21} &= \pi\rho \int_0^l b^2\alpha f_{h_1}(x) f_{h_2}(x)\,dx \\
A_{13} &= \int_0^l S_\alpha f_{h_1}(x) f_\alpha(x)\,dx & C_{13} &= \pi\rho \int_0^l b^3\beta f_{h_1}(x) f_\alpha(x)\,dx \\
A_{22} &= \int_0^l m\left[f_{h_2}(x)\right]^2 dx & C_{22} &= \pi\rho \int_0^l b^2\alpha\left[f_{h_2}(x)\right]^2 dx \\
A_{23} &= \int_0^l S_\alpha f_{h_2}(x) f_\alpha(x)\,dx & C_{23} &= \pi\rho \int_0^l b^3\beta f_{h_2}(x) f_\alpha(x)\,dx \\
A_{31} &= \int_0^l S_\alpha f_{h_1}(x) f_\alpha(x)\,dx & C_{31} &= \pi\rho \int_0^l b^3\gamma f_{h_1}(x) f_\alpha(x)\,dx \\
A_{32} &= \int_0^l S_\alpha f_{h_2}(x) f_\alpha(x)\,dx & C_{32} &= \pi\rho \int_0^l b^3\gamma f_{h_2}(x) f_\alpha(x)\,dx \\
A_{33} &= \int_0^l I_\alpha\left[f_\alpha(x)\right]^2 dx & C_{33} &= \pi\rho \int_0^l b^4\delta\left[f_\alpha(x)\right]^2 dx
\end{aligned}
\qquad (2)
$$

The values ω_{h_1}, ω_{h_2}, and ω_α in equation (1) are, respectively, the angular frequencies of the first bending, second bending, and first torsional modes of vibration. The parameter Ω is a characteristic value given, in terms of the flutter frequency ω and a concept of the structural damping coefficient g, by the relation

$$\Omega = \frac{1}{\omega^2}\left[1 + ig\right] \qquad (3)$$

The functions $f_{h_1}(x)$, $f_{h_2}(x)$, and $f_\alpha(x)$ (equation (2)) refer, respectively, to normalized displacements in the first bending, second, bending, and first torsional modes of vibration of the wing. The quantities α, β, γ, and δ appearing in the C coefficients are functions of the reduced-frequency parameter $\frac{v}{b\omega}$ and may be written in terms of the tabulated aerodynamic coefficients of reference 5 as follows:

$$\left.\begin{aligned} \alpha &= L_h \\ \beta &= L_\alpha - L_h\left(\tfrac{1}{2} + a\right) \\ \gamma &= M_h - L_h\left(\tfrac{1}{2} + a\right) \\ \delta &= M_\alpha - L_\alpha\left(\tfrac{1}{2} + a\right) - M_h\left(\tfrac{1}{2} + a\right) + L_h\left(\tfrac{1}{2} + a\right)^2 \end{aligned}\right\} \quad (4)$$

The flutter speed and frequency are determined from the characteristic values of $\frac{v}{b\omega}$ and ω that cause the flutter determinant (1) to vanish.

RESULTS AND DISCUSSION

As previously pointed out, most of the theoretical results discussed herein are based on analyses in which two-dimensional aerodynamic coefficients were employed. In the case of wings of low aspect ratio these calculations probably are not physically significant but were carried out to show the trends that would be indicated by the two-dimensional aerodynamic theory.

Results of the experimental and theoretical investigations for each model, with sufficient data to permit additional analytical investigations, are given in tables II to X. In these tables, if no theoretical results are given, either no solution existed or none lay within a practical range of values of the parameter $v/b\omega$.

Figures 2 to 10 illustrate, primarily, some effects of variation in density on flutter characteristics for wings of various aspect ratio and with various positions of the center of gravity and elastic axis. In these figures the flutter-speed coefficient $v/b\omega_\alpha$ is plotted against the density parameter $1/\sqrt{\kappa}$, where κ is the ratio of the mass of a cylinder of the surrounding fluid with diameter equal to the chord of the wing to the mass of the wing, both taken for equal lengths along the

span. The experimental results indicate, in general, that a decrease in the parameter $1/\sqrt{\kappa}$ results in a decrease in the flutter-speed coefficient. Over most of the range of values of the parameter $1/\sqrt{\kappa}$ the flutter-speed coefficient is nearly proportional to the inverse of the square root of the density. In some cases, however, for values of $1/\sqrt{\kappa}$ less than 2, a minimum value of the experimentally determined flutter-speed coefficient is indicated and a slight increase in the flutter-speed coefficient is noted. (See figs. 2 and 3.) (The theoretical curves based on two modal functions in figure 3 are discussed in detail subsequently.) For the higher values of the relative-density parameter $\left(1/\sqrt{\kappa}\right.$ greater than 3$\left.\right)$ the results of the analysis based on two-dimensional aerodynamic data generally follow the trends indicated by experiment but are conservative. Near a value of $1/\sqrt{\kappa}$ slightly less than 3, however, the analytical considerations employed predict a minimum value of the flutter-speed coefficient after which an abrupt increase is indicated. Experimental points were obtained below this minimum theoretical value of the flutter-speed coefficient. At still lower values of $1/\sqrt{\kappa}$ the analytical considerations employed showed freedom from flutter. Further analytical investigation of this region therefore appears desirable.

The data of figures 2 to 10 have been replotted in figure 11 to illustrate the effect of decreasing the semispan-chord ratio. Each of these figures is related to wings of constant section properties but differing in span. As stated previously, the calculations of the theoretical curves shown in these figures were based on two-dimensional air-force coefficients and, although they probably are not physically significant for the wings of lower aspect ratio, were carried out to show the trends that would be indicated by the two-dimensional aerodynamic theory. In figure 11 the results based on the two-dimensional aerodynamic theory are seen to fit in fairly well with experimental data for the wings of highest aspect ratio except at low values of the relative-density parameter. Greater deviations between experiment and the two-dimensional aerodynamic theory are shown, however, as the aspect ratio is decreased.

In a few selected cases corrections for the effects of finite span were applied by the method of reference 3 to a wing of aspect ratio 6 (model 17-32-3). In order to simplify the analytical procedure only two uncoupled modes, namely, linear torsion and parabolic bending, were employed. A comparison with the results of two-dimensional aerodynamic theory was provided by using these same two modal functions in an analysis based on two-dimensional air forces. The results of these calculations are shown in figure 3. A comparison of the results indicates that the application of finite-span corrections provides good agreement with experiment for high values of the relative-density parameter but has little effect in the region of low values of this parameter where the two-dimensional aerodynamic theory predicts an abrupt rise in the flutter-speed coefficient.

In conjunction with the question of a minimum value of the flutter-speed coefficient associated with the discussion of the theoretical results shown in figures 2 to 11, figure 12 is presented to illustrate the form of the conventional plot of the damping coefficient g against the wave-length parameter $v/b\omega$ for several points selected from the theoretical curve shown in figure 3. The plots are arranged in order of decreasing values of the parameter $1/\sqrt{\kappa}$. Where instability was indicated, flutter conditions were obtained for the case $g = 0$. Note that, as $1/\sqrt{\kappa}$ is decreased, a borderline condition between stability and instability is approached (fig. 12(d)). This condition, together with the flutter-free condition indicated for still lower values of $1/\sqrt{\kappa}$ (figs. 12(e) and 12(f)), is consistent with the existence of a minimum value of the flutter-speed coefficient shown in figures 2 to 11. Of the three characteristic values satisfying the flutter determinant the only one plotted in figure 12 is that for which the associated frequency approached the experimentally determined flutter frequency. Increasingly negative values of g with increasing values of $v/b\omega$ were found for the other characteristic values over the range of $v/b\omega$ considered. An indication that the consideration of additional degrees of freedom in the analysis would not have altered these results appreciably can be gained from the fact that the differential-equation approach of reference 6 was applied to a case similar to that represented by figure 12(e) and no solution was obtained within a reasonable range of values of $v/b\omega$.

Figures 13 to 17 show the dynamic pressure at flutter as a function of the wave-length parameter $v/b\omega$. The theoretical values of dynamic pressure shown in the figures are those which arise from the calculations based on incompressible aerodynamic forces. The experimental values have been modified by the compressibility factor $1/\sqrt{1 - M^2}$, as was done in reference 1, to permit comparison with the theoretical values. The figures indicate that the dynamic pressure at flutter remains essentially constant with decreasing wave length until a low critical value of $v/b\omega$ (generally near 2) is reached. At this point a sudden rise in dynamic pressure occurs. Examination of figures 13, 14, and 15, which relate to wings of equivalent section properties but differing in semispan-chord ratio, indicates that as the semispan-chord ratio is decreased, the value of the wave-length parameter at which the abrupt rise in dynamic pressure occurs is decreased and the spread between experiment and the analytical results based on two-dimensional aerodynamic theory is increased.

It should be noted that the type of wing construction employed permits the possibility of fore and aft (that is, in the stream direction) bending entering the problem. The effects of fore and aft bending were, however, not considered in the analytical work.

CONCLUSIONS

An experimental investigation has been made of some effects of variations in several parameters, including fluid density, on the flutter characteristics of light uniform cantilever wings. The assortment of wings covered a variety of positions of the elastic axis and center of gravity and values of the aspect ratio of 8, 6, and 4. The relative-density parameter $1/\sqrt{\kappa}$ was varied over a range of values from 1.2 to nearly 14. The experimental investigation has been supplemented by an analytical investigation based, for most cases, on two-dimensional aerodynamic theory for incompressible flow. Corrections for effects of finite span have been made to selected data. The results presented support the following conclusions:

1. The general experimental and analytical investigations confirmed the observation that, for fairly high values of the relative-density parameter ($1/\sqrt{\kappa}$ greater than 3), the flutter-speed coefficient decreased with decreasing values of the relative-density parameter and was nearly proportional to the inverse of the square root of the air density.

2. For fairly high values of the relative-density parameter ($1/\sqrt{\kappa}$ greater than 3), the results of the analysis based on two-dimensional aerodynamic data generally followed the trends indicated by experiment but were conservative.

3. For lower values of the relative-density parameter ($1/\sqrt{\kappa}$ less than 3), the trends of the two-dimensional aerodynamic theory indicated a minimum value of, and an abrupt rise in, the value of the flutter-speed coefficient, whereas, experimental points were obtained below this minimum theoretical value. A region exists, then, where the analytical considerations employed indicated a freedom from flutter not supported by experiment. Further analytical investigation of this region seems desirable.

4. The application of finite-span corrections to results for one configuration improved the agreement with experiment for high values of the relative-density parameter but showed little effect in the region of low values of this parameter where the two-dimensional aerodynamic theory predicted an abrupt rise in the flutter-speed coefficient.

5. The dynamic pressure at flutter, with experimental values modified by a compressibility correction, was in general, relatively constant for values of the wave-length parameter $v/b\omega$ greater than 2 or 3.

Langley Aeronautical Laboratory
National Advisory Committee for Aeronautics
Langley Field, Va., September 6, 1951

REFERENCES

1. Castile, George E., and Herr, Robert W.: Some Effects of Density and Mach Number on the Flutter Speed of Two Uniform Wings. NACA TN 1989, 1949.

2. Theodorsen, Theodore, and Garrick, I. E.: Mechanism of Flutter — A Theoretical and Experimental Investigation of the Flutter Problem. NACA Rep. 685, 1940.

3. Reissner, Eric, and Stevens, John E.: Effect of Finite Span on the Airload Distributions for Oscillating Wings. II - Methods of Calculation and Examples of Application. NACA TN 1195, 1947.

4. Scanlan, Robert H., and Rosenbaum, Robert: Introduction to the Study of Aircraft Vibration and Flutter. The Macmillan Co., 1951.

5. Smilg, Benjamin, and Wasserman, Lee S.: Application of Three-Dimensional Flutter Theory to Aircraft Structures. ACTR No. 4798, Materiel Div., Army Air Corps, July 9, 1942.

6. Runyan, Harry L., and Watkins, Charles E.: Flutter of a Uniform Wing with an Arbitrarily Placed Mass According to a Differential-Equation Analysis and a Comparison with Experiment. NACA Rep. 966, 1950. (Formerly NACA TN 1848.)

TABLE I.- CHARACTERISTICS OF MODELS

Model	a	$a + x_\alpha$	r_α^2	GJ (lb-in.^{2})	EI (lb-in.^{2})	ω_{h_1} (radians/sec)	ω_{h_2} (radians/sec)	ω_α (radians/sec)	m (slugs/ft)
17-32-4	-0.628	-0.358	0.336	15,400	180,600	75.7	481.7	136.0	0.0106
17-32-3	-.628	-.358	.336	15,400	180,600	134.5	855.9	181.6	.0106
17-32-2	-.628	-.358	.336	15,400	180,600	302.5	1925.0	272.0	.0106
27-38-4	-.454	-.242	.258	25,720	264,000	80.4	511.6	178.0	.0135
27-38-3	-.454	-.242	.258	25,720	264,000	142.5	906.7	237.0	.0135
27-38-2	-.454	-.242	.258	25,720	264,000	321.4	2045.0	355.0	.0135
27-31-4	-.454	-.374	.256	25,720	264,000	70.4	448.0	155.0	.0167
39-42-4	-.218	-.150	.162	22,200	236,000	96.1	612.0	232.0	.0132
39-42-3	-.218	-.150	.162	22,200	236,000	170.6	1086.0	310.0	.0132

TABLE II.- EXPERIMENTAL AND THEORETICAL DATA FOR MODEL 17-32-4

$\frac{1}{\sqrt{\kappa}}$	M	Experiment				Theory			
		$v/b\omega_\alpha$	ω/ω_α	$v/b\omega$	$q/\sqrt{1 - M^2}$ (lb/sq ft)	$v/b\omega_\alpha$	ω/ω_α	$v/b\omega$	q (lb/sq ft)
Air									
2.36	0.126	2.06	0.809	2.54	20.1	2.26	0.840	2.69	24.0
3.01	.151	2.47	.813	3.04	22.6	2.34	.836	2.80	20.1
3.25	.165	2.69	.802	3.36	21.6	2.50	.859	2.91	17.4
3.75	.182	2.96	.798	3.71	19.7	2.63	.822	3.20	15.3
4.62	.219	3.56	.799	4.46	22.7	3.21	.807	3.98	15.0
5.32	.242	3.93	.784	5.02	17.5	3.47	.782	4.44	13.2
6.19	.271	4.40	.768	5.74	16.3	4.18	.764	5.47	14.1
7.05	.306	4.95	.760	6.52	16.1	4.51	.803	5.62	12.7
8.42	.356	5.74	.754	7.62	15.5	5.46	.783	6.97	13.1
Freon-12									
1.20	0.222	1.63	0.803	2.03	58.5	----	-----	----	----
1.33	.208	1.53	.785	1.95	41.9	----	-----	----	----
1.48	.210	1.57	.810	1.94	35.5	----	-----	----	----
1.73	.222	1.66	.826	2.01	29.5	----	-----	----	----
2.14	.262	1.97	.947	2.08	27.5	2.31	0.840	2.75	36.0
3.01	.325	2.51	.828	3.03	22.9	2.37	.840	2.82	19.2

TABLE III.- EXPERIMENTAL AND THEORETICAL DATA FOR

MODEL 17-32-3

$\frac{l}{\sqrt{\kappa}}$	M	Experiment				Theory			
		$v/b\omega_\alpha$	ω/ω_α	$v/b\omega$	$q/\sqrt{1 - M^2}$ (lb/sq ft)	$v/b\omega_\alpha$	ω/ω_α	$v/b\omega$	q (lb/sq ft)
Air									
2.42	0.155	1.92	0.936	2.05	35.4	1.77	0.964	1.84	29.6
2.96	.184	2.28	.939	2.42	33.4	1.92	.960	2.00	23.3
3.40	.210	2.60	.944	2.76	33.3	2.10	.966	2.18	21.2
4.22	.252	3.11	.930	3.34	31.1	2.39	.992	2.41	17.8
4.73	.277	3.41	.921	3.70	29.9	2.74	.942	2.91	18.5
5.52	.313	3.85	.917	4.20	28.3	3.06	.947	3.23	17.0
6.47	.110	1.36	.687	1.98	2.45	3.55	.922	3.85	16.7
7.63	.144	1.78	.698	2.56	3.06	3.97	.906	4.38	15.0
Freon-12									
1.20	0.311	1.66	0.949	1.75	111.9	----	-----	----	-----
1.45	.299	1.60	.930	1.72	70.6	----	-----	----	-----
1.68	.302	1.63	.959	1.70	54.2	3.22	1.00	3.22	202.6
2.11	.330	1.80	.948	1.90	42.8	1.81	.963	1.88	40.8
2.46	.358	1.99	.952	2.09	39.0	1.77	.962	1.84	28.9
2.78	.392	2.19	.948	2.31	37.4	1.84	.964	1.91	24.3
3.46	.455	2.55	.930	2.74	33.8	2.13	.968	2.20	21.1

TABLE IV.- EXPERIMENTAL AND THEORETICAL DATA FOR

MODEL 17-32-2

$\frac{1}{\sqrt{\kappa}}$	M	Experiment				Theory			
		$v/b\omega_\alpha$	ω/ω_α	$v/b\omega$	$q/\sqrt{1 - M^2}$ (lb/sq ft)	$v/b\omega_\alpha$	ω/ω_α	$v/b\omega$	q (lb/sq ft)
Air									
2.44	0.212	1.75	1.151	1.52	66.1	1.42	1.291	1.10	49.0
2.99	.252	2.09	1.118	1.87	62.8	1.47	1.278	1.15	30.1
3.33	.285	2.35	1.152	2.04	64.8	1.51	1.302	1.16	25.7
4.26	.351	2.89	1.194	2.42	61.3	1.69	1.310	1.29	19.6
4.97	.405	3.33	1.224	2.72	61.3	2.04	1.308	1.56	21.4
5.62	.458	3.76	1.205	3.12	62.8	2.61	1.292	2.02	26.8
6.25	.507	4.17	1.234	3.38	64.3	2.98	1.124	2.65	28.3
7.15	.577	4.72	1.232	3.83	66.2	3.30	1.196	2.76	26.5
8.55	.683	5.59	1.210	4.62	72.8	4.13	1.236	3.34	29.1
9.54	.737	6.02	1.209	4.98	73.5	4.52	1.208	3.74	28.0

TABLE V.- EXPERIMENTAL AND THEORETICAL DATA FOR

MODEL 27-38-4

$\frac{1}{\sqrt{\kappa}}$	M	Experiment				Theory			
		$v/b\omega_\alpha$	ω/ω_α	$v/b\omega$	$q/\sqrt{1 - M^2}$ (lb/sq ft)	$v/b\omega_\alpha$	ω/ω_α	$v/b\omega$	q (lb/sq ft)
Air									
2.76	0.151	1.93	0.748	2.58	33.6	1.83	0.712	2.57	30.1
3.22	.171	2.18	.744	2.93	31.4	2.02	.709	2.85	26.7
3.95	.204	2.59	.728	3.56	29.8	2.34	.703	3.33	23.9
5.42	.268	3.40	.677	5.02	27.7	3.02	.692	4.37	21.1
8.00	.387	4.88	.642	7.60	27.4	-----	-----	-----	-----
10.59	.484	6.06	.614	9.88	25.4	5.38	.727	7.40	17.6
12.91	.587	7.29	.595	12.25	26.8	6.40	.694	9.23	16.7
13.81	.594	7.36	.595	12.36	24.0	6.71	.638	10.52	16.1
Freon-12									
1.36	0.220	1.23	0.699	1.76	56.1	-----	-----	-----	-----
1.46	.227	1.25	.727	1.72	50.9	-----	-----	-----	-----
1.64	.236	1.30	.726	1.79	44.1	10.98	0.594	18.50	303.6
1.91	.261	1.45	.740	1.96	40.5	1.70	.711	2.39	54.1
2.38	.297	1.68	.764	2.20	35.5	1.72	.714	2.41	35.5
3.50	.393	2.32	.739	3.14	32.3	2.15	.707	3.04	25.6

TABLE VI.- EXPERIMENTAL AND THEORETICAL DATA FOR MODEL 27-38-3

$\frac{1}{\sqrt{\kappa}}$	M	Experiment				Theory			
		$v/b\omega_\alpha$	ω/ω_α	$v/b\omega$	$q\sqrt{1 - M^2}$ (lb/sq ft)	$v/b\omega_\alpha$	ω/ω_α	$v/b\omega$	q (lb/sq ft)
Air									
2.76	0.204	1.94	0.789	2.46	60.7	----	-----	----	----
3.45	.252	2.39	.733	2.26	62.9	1.84	0.814	2.26	36.1
3.94	.287	2.72	.724	3.76	60.1	2.05	.810	2.53	32.7
4.78	.342	3.23	.695	4.65	58.4	2.39	.802	2.98	30.1
5.73	.398	3.75	.734	5.11	56.2	2.76	.801	3.45	28.1
7.81	.481	4.50	.773	5.82	45.7	3.08	.830	3.71	18.7
9.85	.622	5.36	.724	7.99	53.0	4.34	.747	5.81	23.4
Freon-12									
1.53	0.303	1.30	0.770	1.69	91.4	----	-----	----	----
1.98	.346	1.49	.748	1.91	72.7	----	-----	----	----
2.45	.389	1.67	.777	2.15	60.9	1.56	0.817	1.91	48.7
2.75	.426	1.84	.770	2.39	59.4	1.64	.816	2.01	42.5
3.04	.462	2.00	.695	2.88	58.7	1.65	.782	2.11	35.3
3.39	.508	2.20	.736	2.99	59.1	1.85	.815	2.27	36.1
4.13	.572	2.47	.714	3.46	55.4	2.08	.810	2.57	32.3

TABLE VII.- EXPERIMENTAL AND THEORETICAL DATA FOR

MODEL 27-38-2

$\frac{l}{\sqrt{\kappa}}$	M	Experiment				Theory			
		$v/b\omega_\alpha$	ω/ω_α	$v/b\omega$	$q/\sqrt{1 - M^2}$ (lb/sq ft)	$v/b\omega_\alpha$	ω/ω_α	$v/b\omega$	q (lb/sq ft)
Air									
2.78	0.279	1.77	0.922	1.92	114.1	1.32	1.065	1.24	61.0
3.41	.335	2.12	.888	2.39	110.5	1.48	1.072	1.38	51.2
3.93	.349	2.21	.948	2.33	90.6	1.65	1.086	1.52	47.1
4.91	.445	2.80	.886	3.16	98.2	1.98	1.064	1.86	44.1
5.95	.525	3.28	.872	3.76	96.7	2.37	1.049	2.26	42.7
7.10	.623	3.83	.855	4.48	100.7	2.88	1.014	2.84	44.5
8.33	.704	4.30	.833	5.16	101.4	3.23	1.070	3.02	40.5
10.08	.835	5.05	.778	6.49	123.5	3.77	1.030	3.66	37.9
Freon-12									
4.53	0.723	2.12	0.800	2.65	85.7	1.85	1.069	1.73	44.9

TABLE VIII.- EXPERIMENTAL AND THEORETICAL DATA FOR MODEL 27-31-4

$\frac{1}{\sqrt{\kappa}}$	M	Experiment				Theory			
		$v/b\omega_\alpha$	ω/ω_α	$v/b\omega$	$q/\sqrt{1-M^2}$ (lb/sq ft)	$v/b\omega_\alpha$	ω/ω_α	$v/b\omega$	q (lb/sq ft)
Air									
3.01	0.177	2.56	0.676	3.79	46.2	3.04	0.671	4.53	63.9
3.70	.210	3.02	.674	4.48	43.2	3.25	.668	4.87	48.8
4.38	.242	3.47	.672	5.17	40.9	3.60	.667	5.40	42.5
5.17	.281	4.02	.664	6.06	39.7	3.96	.671	5.90	36.9
5.53	.310	4.44	.664	6.69	42.6	4.25	.656	6.48	37.2
6.71	.353	5.05	.656	7.70	38.2	5.03	.657	7.66	35.4
7.36	.385	5.49	.633	8.68	38.0	5.44	.654	8.32	34.4
8.20	.423	6.01	.633	9.49	37.3	5.99	.648	9.25	33.7
9.67	.477	6.75	.628	10.76	35.0	6.93	.646	10.72	32.4
Freon-12									
1.80	0.289	1.83	0.683	2.68	66.4	----	-----	-----	----
2.10	.315	1.98	.705	2.81	59.3	----	-----	-----	----
2.63	.346	2.20	.675	3.26	47.4	3.14	0.671	4.68	89.9
3.21	.394	2.55	.692	3.69	43.4	3.08	.671	4.59	57.9
3.82	.442	2.90	.686	4.23	40.5	3.30	.668	4.94	47.0
4.90	.518	3.49	.715	4.88	37.5	3.92	.666	5.89	40.4

NACA

TABLE IX.- EXPERIMENTAL AND THEORETICAL DATA FOR MODEL 39-42-4

$\frac{l}{\sqrt{\kappa}}$	M	Experiment				Theory			
		$v/b\omega_\alpha$	ω/ω_α	$v/b\omega$	$q\sqrt{1-M^2}$ (lb/sq ft)	$v/b\omega_\alpha$	ω/ω_α	$v/b\omega$	q (lb/sq ft)
Air									
2.63	0.146	1.39	0.563	2.47	32.1	1.42	0.606	2.34	33.0
3.24	.177	1.68	.524	3.21	31.0	1.60	.603	2.66	27.7
3.63	.197	1.89	.532	3.55	30.6	1.73	.602	2.88	25.8
4.18	.222	2.10	.540	3.89	29.3	1.93	.596	3.23	24.1
5.13	.266	2.50	.560	4.47	28.0	2.28	.591	3.86	22.3
6.00	.306	2.88	.542	5.31	27.3	2.61	.572	4.48	21.3
7.35	.365	3.42	.542	6.31	26.3	3.11	.566	5.49	20.2
8.64	.418	3.91	.542	7.22	25.4	3.59	.558	6.43	19.5
10.52	.485	4.51	.539	8.37	23.7	4.29	.549	7.82	18.8
Freon-12									
1.65	0.216	0.94	-----	----	38.0	----	-----	----	----
1.98	.234	1.04	-----	----	32.4	1.37	0.598	2.29	23.4
2.47	.274	1.24	-----	----	29.7	1.38	.605	2.28	29.7
2.79	.300	1.37	-----	----	28.5	1.46	.604	2.42	28.5
3.29	.340	1.58	-----	----	27.9	1.62	.602	2.69	27.9
4.13	.394	1.91	-----	----	26.3	1.92	.598	3.21	26.3

TABLE X.- EXPERIMENTAL AND THEORETICAL DATA FOR

MODEL 39-42-3

$\frac{1}{\sqrt{\kappa}}$	M	Experiment				Theory			
		$v/b\omega_\alpha$	ω/ω_α	$v/b\omega$	$q\sqrt{1 - M^2}$ (lb/sq ft)	$v/b\omega_\alpha$	ω/ω_α	$v/b\omega$	q (lb/sq ft)
Air									
1.60	0.306	0.96	0.644	1.49	77.1	----	-----	----	-----
1.91	.316	1.00	.645	1.55	58.9	1.82	0.675	2.70	184.0
2.39	.353	1.14	.644	1.77	49.2	1.35	.687	1.96	64.2
2.91	.399	1.31	.645	2.03	44.3	1.42	.694	2.04	47.9
3.85	.478	1.58	.627	2.52	38.8	1.66	.692	2.40	37.5

NACA

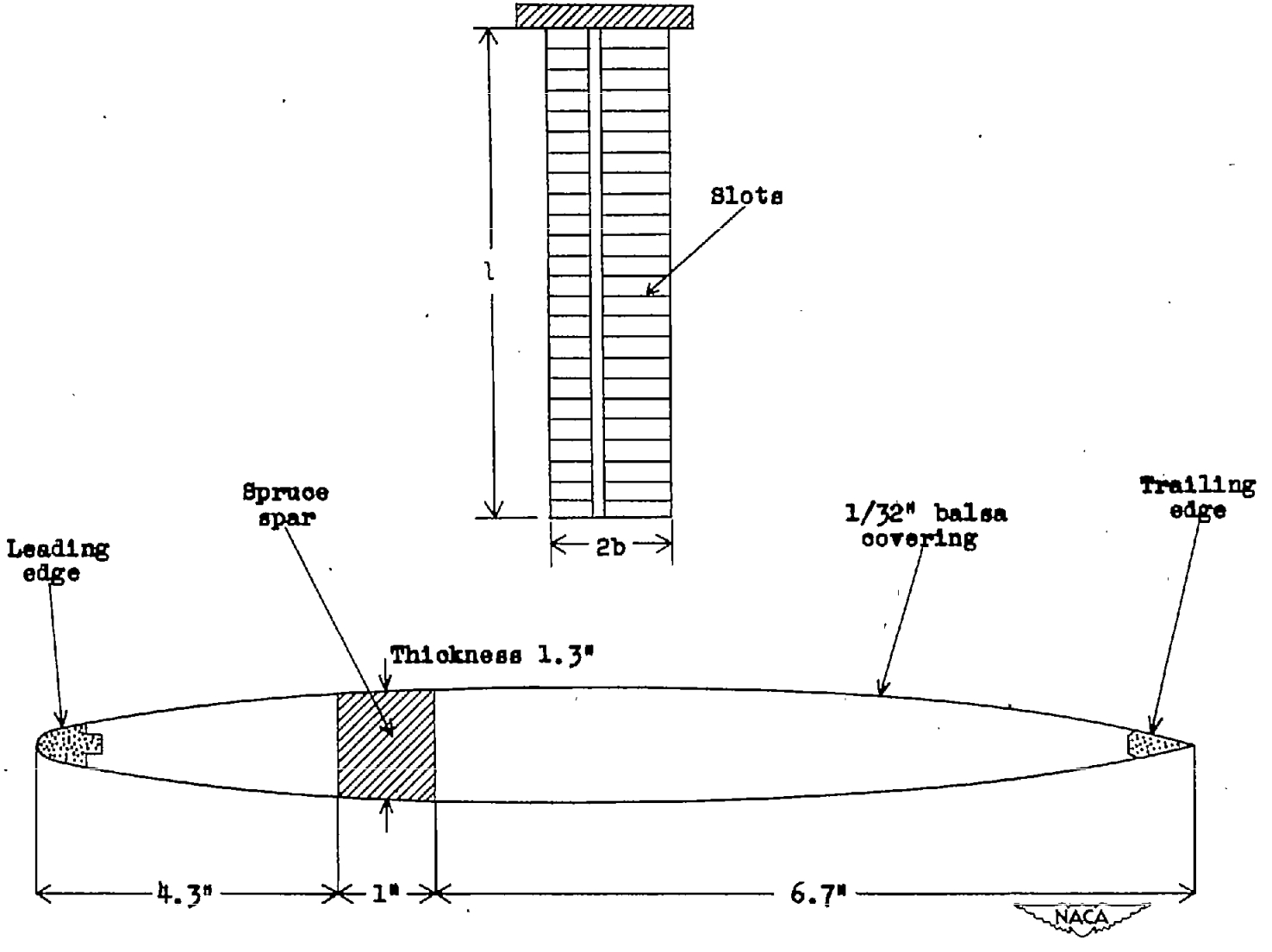

Figure 1.- Plan and cross-sectional views of a typical model (30-percent-spar position from leading edge).

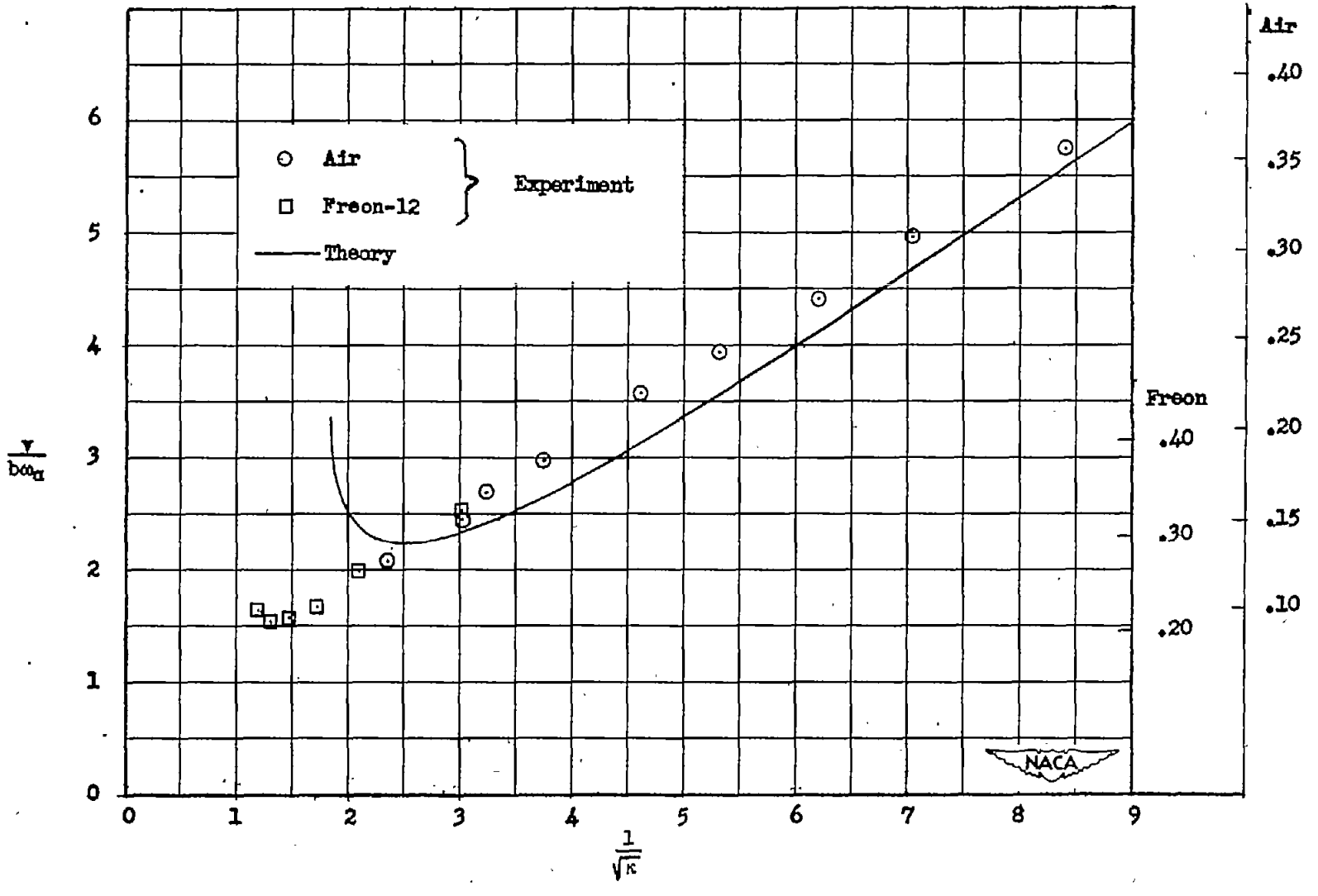

Figure 2.- Variation of flutter-speed coefficient $v/b\omega_\alpha$ with the relative-density parameter $1/\sqrt{\kappa}$ for model 17-32-4.

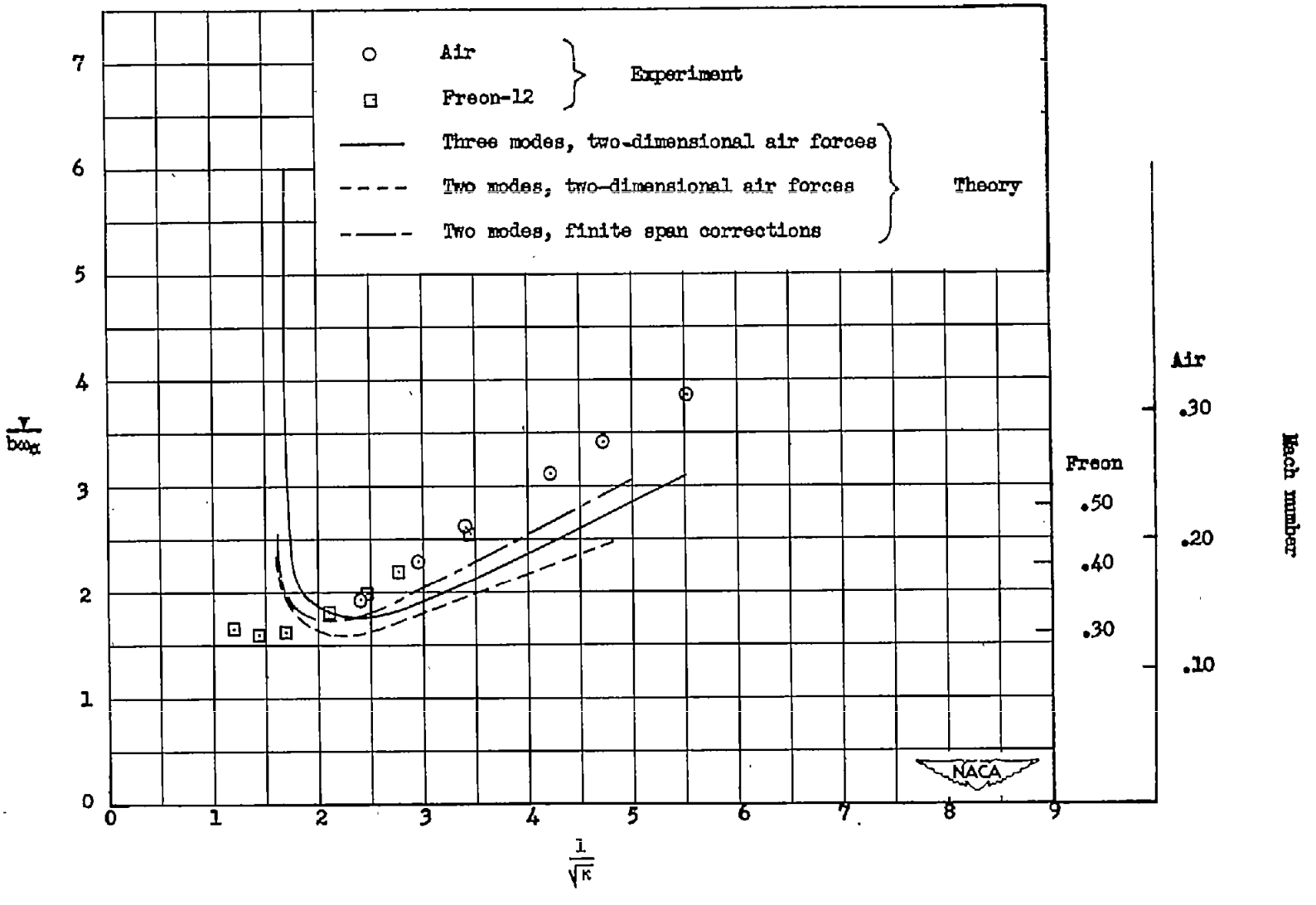

Figure 3.- Variation of flutter-speed coefficient $v/b\omega_\alpha$ with the relative-density parameter $1/\sqrt{\kappa}$ for model 17-32-3.

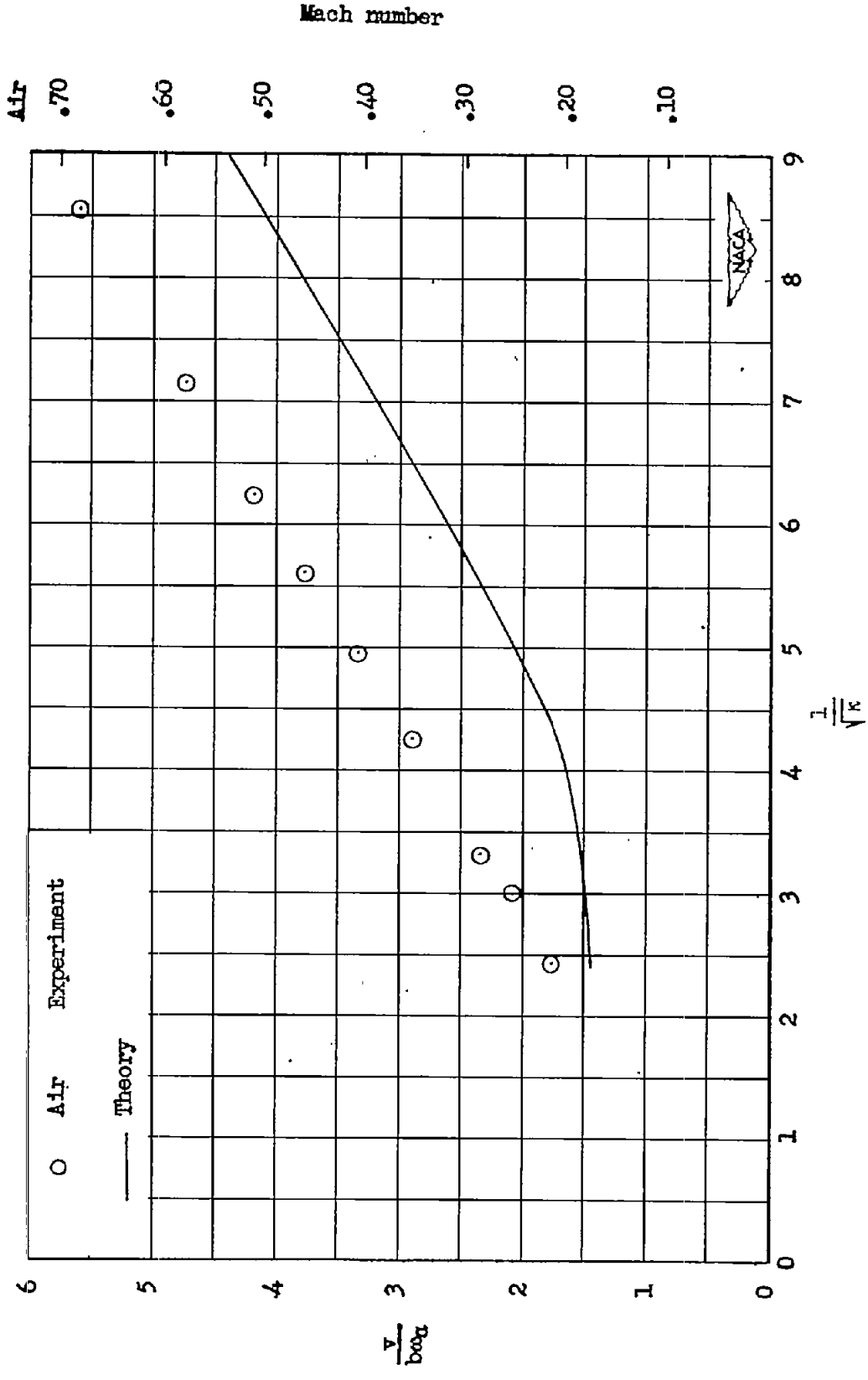

Figure 4.- Variation of flutter-speed coefficient $v/b\omega_\alpha$ with the relative-density parameter $1/\sqrt{\kappa}$ for model 17-32-2.

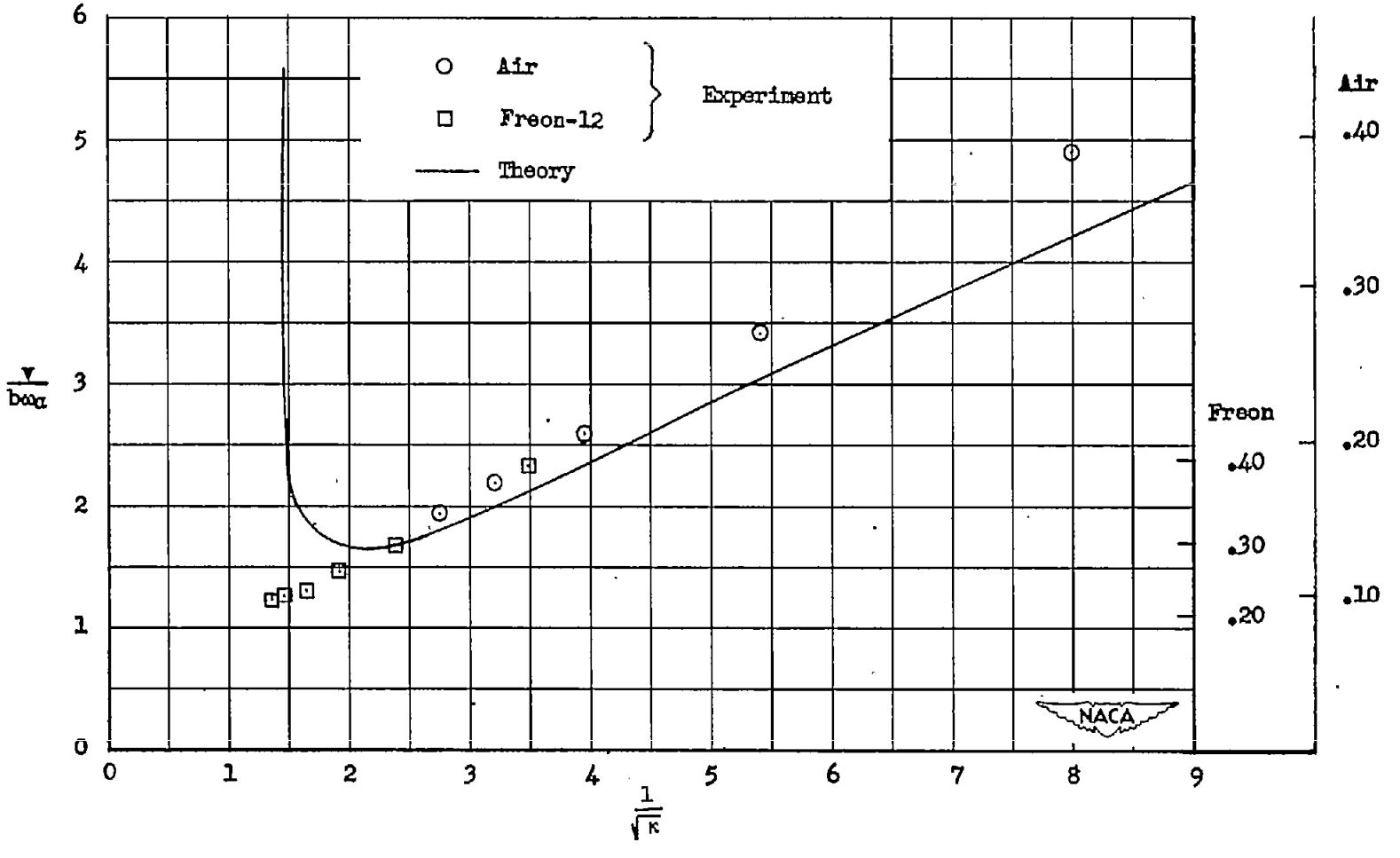

Figure 5.- Variation of flutter-speed coefficient $v/b\omega_\alpha$ with the relative-density parameter $1/\sqrt{\kappa}$ for model 27-38-4.

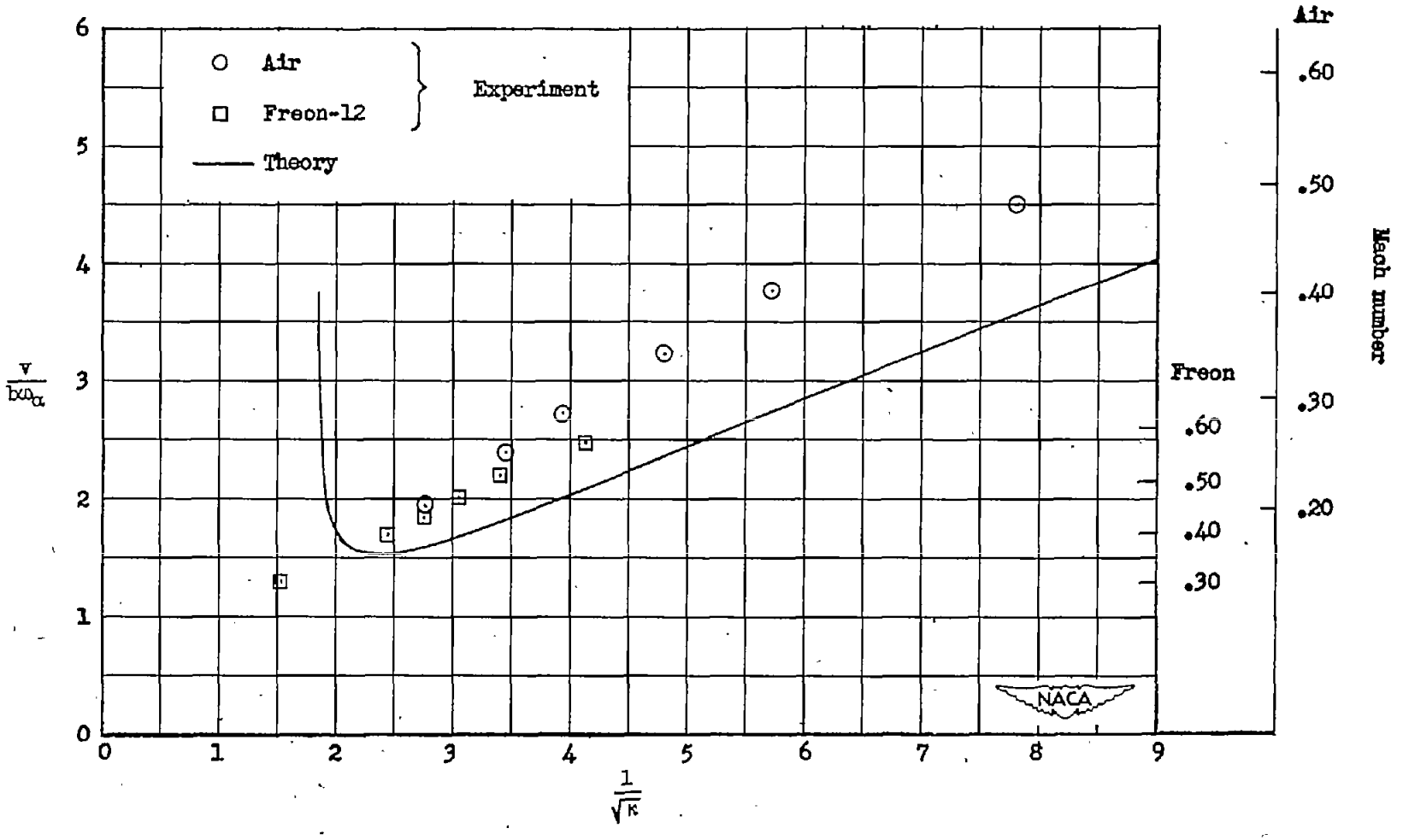

Figure 6.- Variation of flutter-speed coefficient $v/b\omega_\alpha$ with the relative-density parameter $1/\sqrt{\kappa}$ for model 27-38-3.

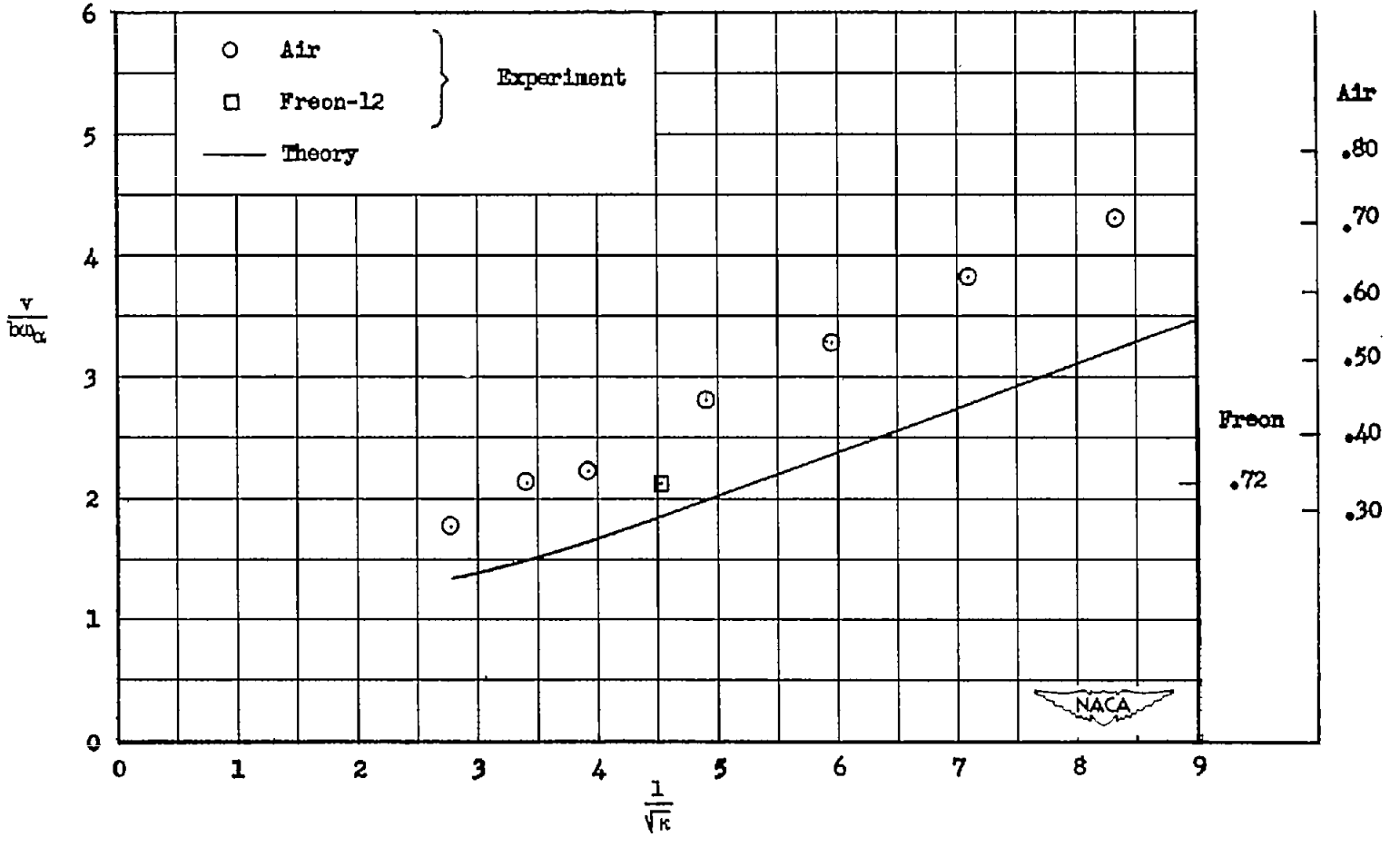

Figure 7.- Variation of flutter-speed coefficient $v/b\omega_\alpha$ with the relative-density parameter $1/\sqrt{\mu}$ for model 27-38-2.

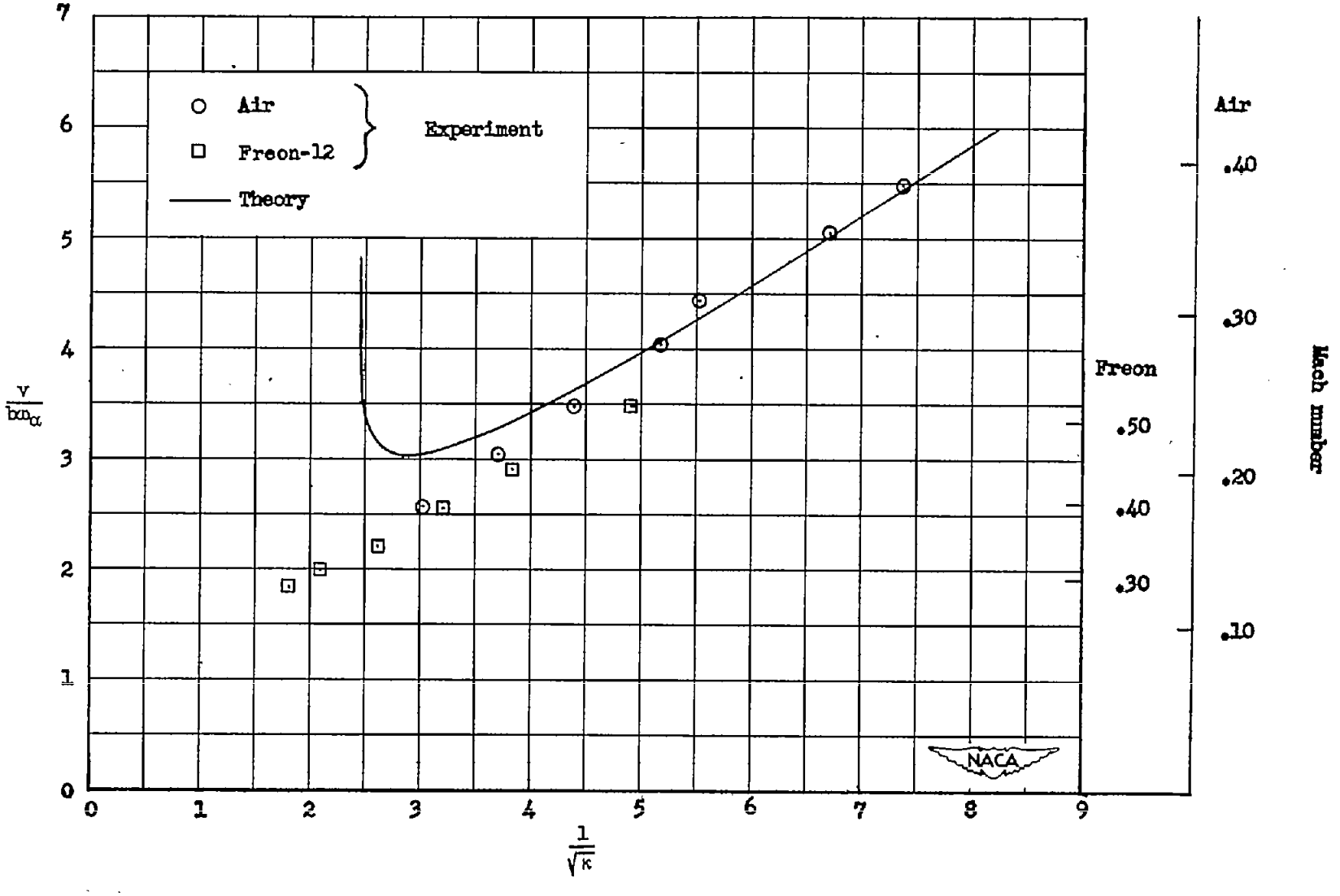

Figure 8.- Variation of flutter-speed coefficient $v/b\omega_\alpha$ with the relative-density parameter $1/\sqrt{\kappa}$ for model 27-31-4.

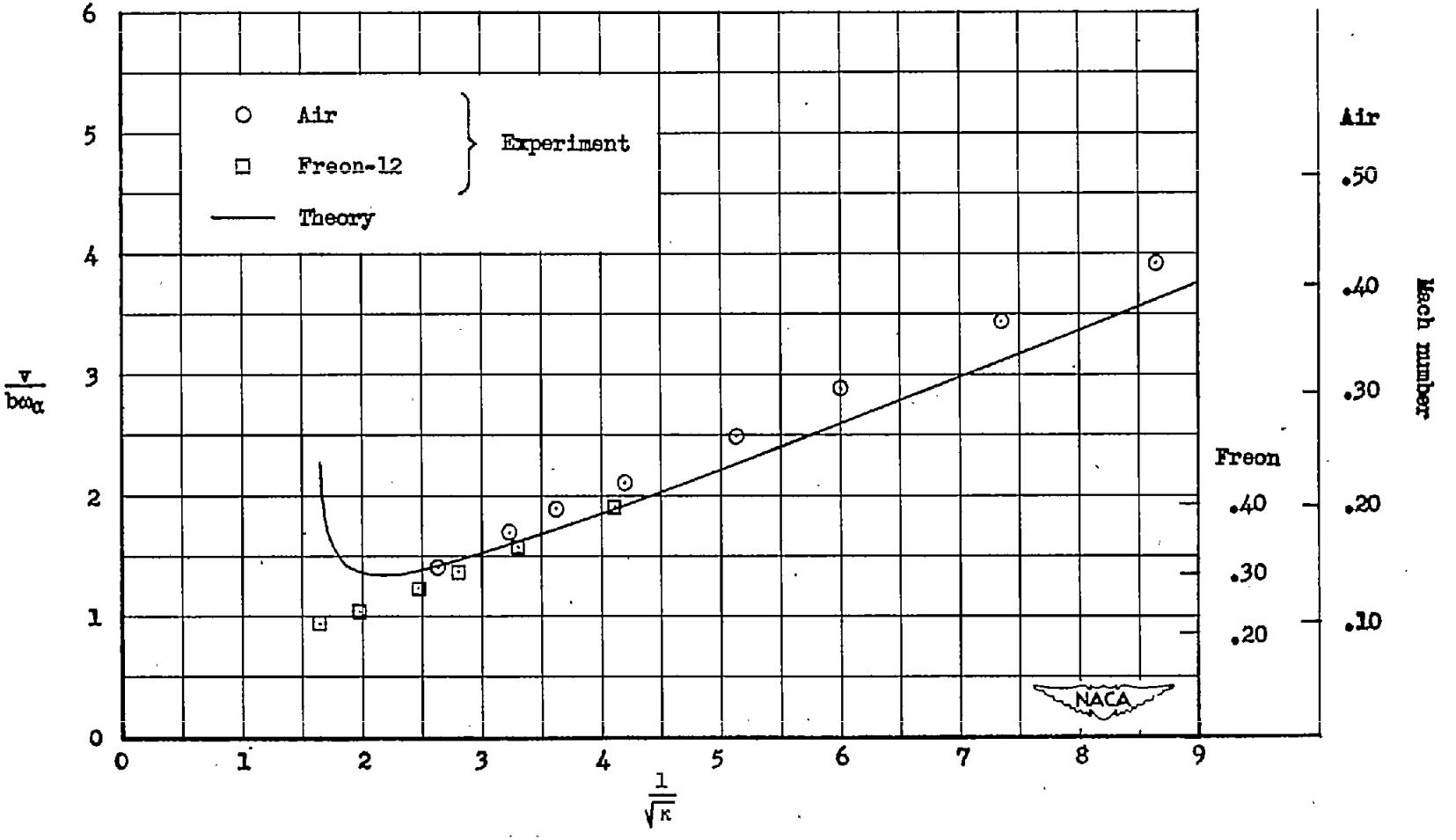

Figure 9.- Variation of flutter-speed coefficient $v/b\omega_\alpha$ with the relative-density parameter $1/\sqrt{\kappa}$ for model 39-42-4.

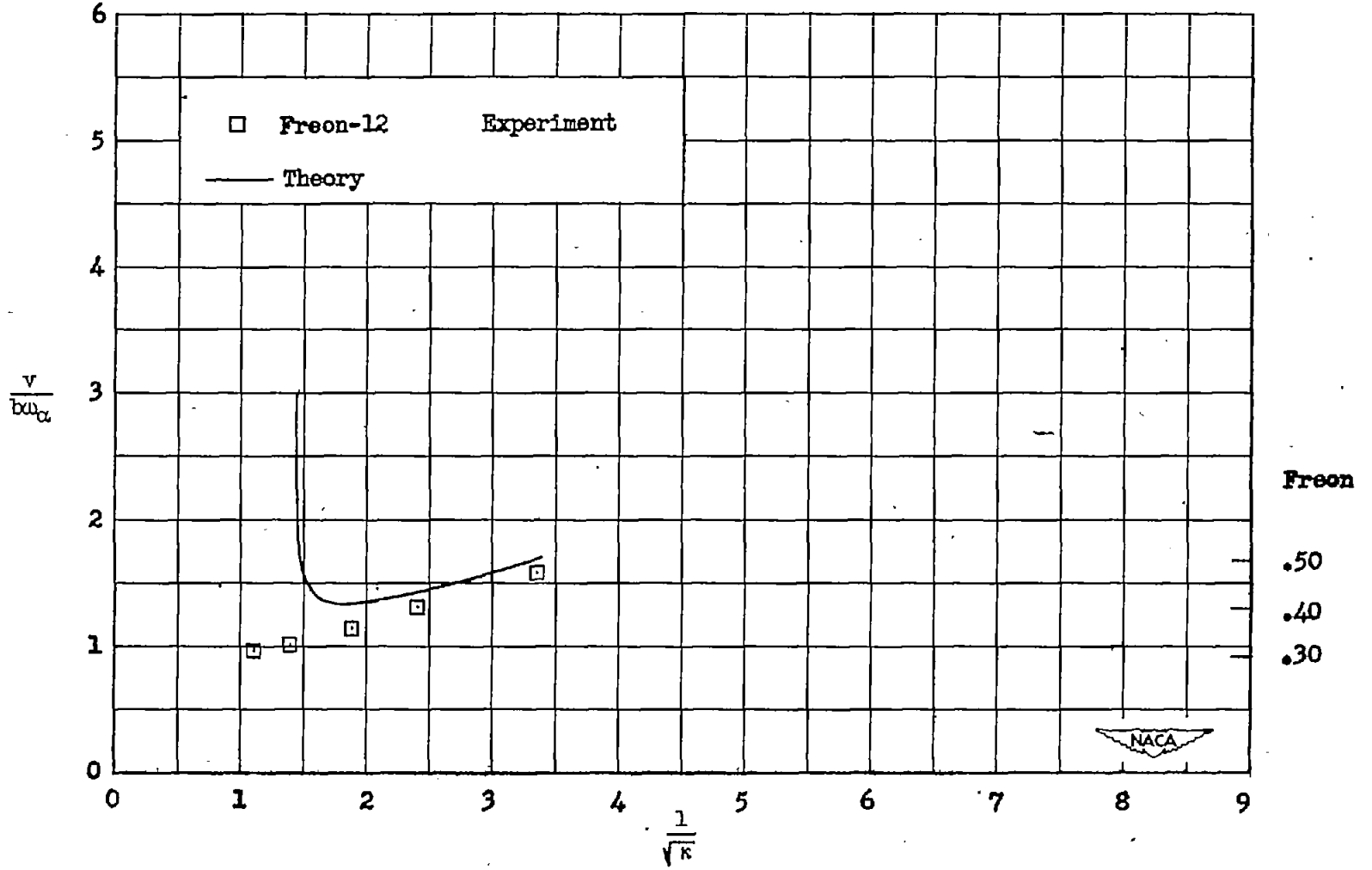

Figure 10.- Variation of flutter-speed coefficient $v/b\omega_\alpha$ with the relative-density parameter $1/\sqrt{\kappa}$ for model 39-42-3.

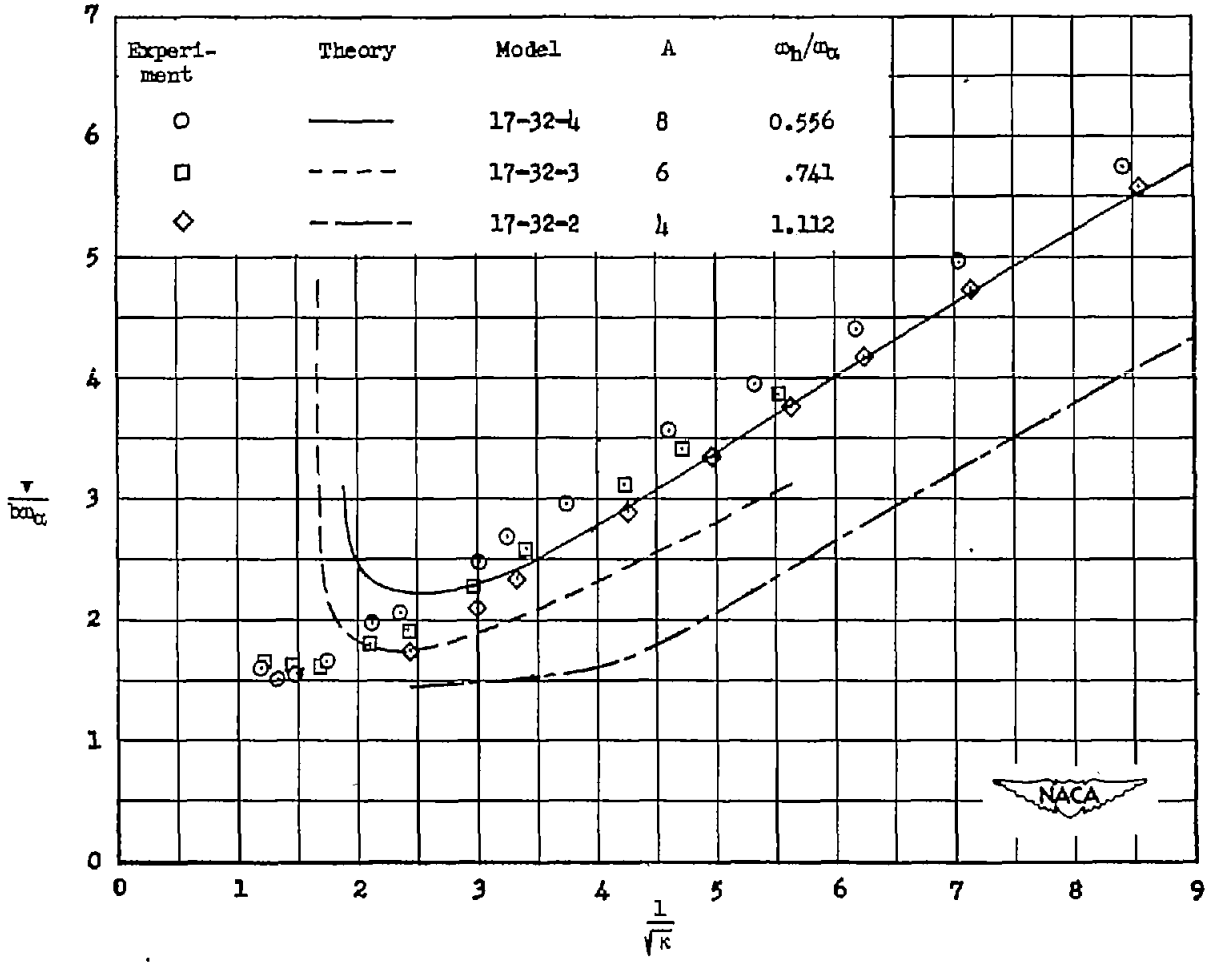

(a) Models 17-32-4, 17-32-3, and 17-32-2.

Figure 11.- Variation of flutter-speed coefficient $V/b\omega_\alpha$ with the relative-density parameter $l/\sqrt{\kappa}$ for models with various l/c ratios.

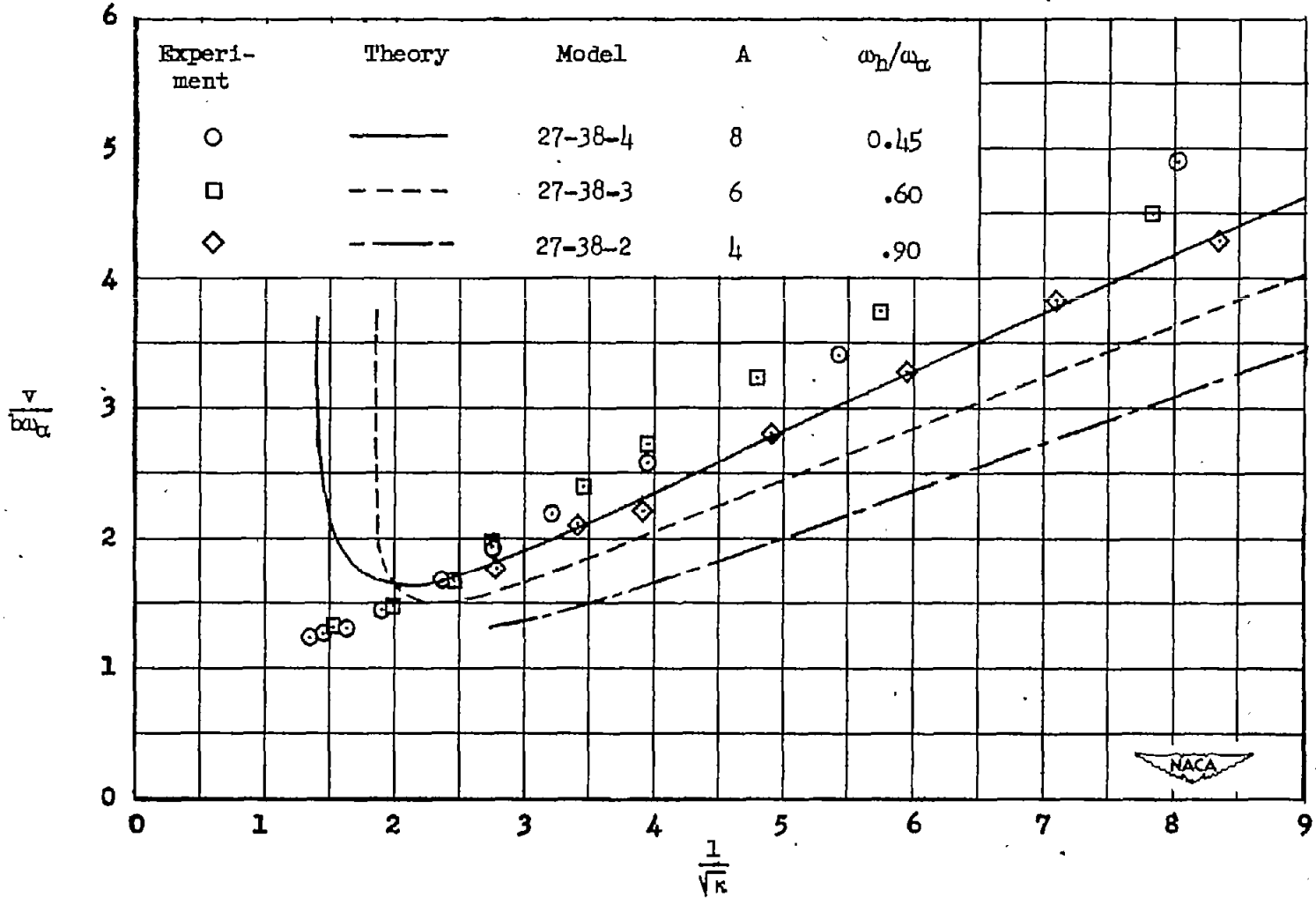

(b) Models 27-38-4, 27-38-3, and 27-38-2.

Figure 11.- Continued.

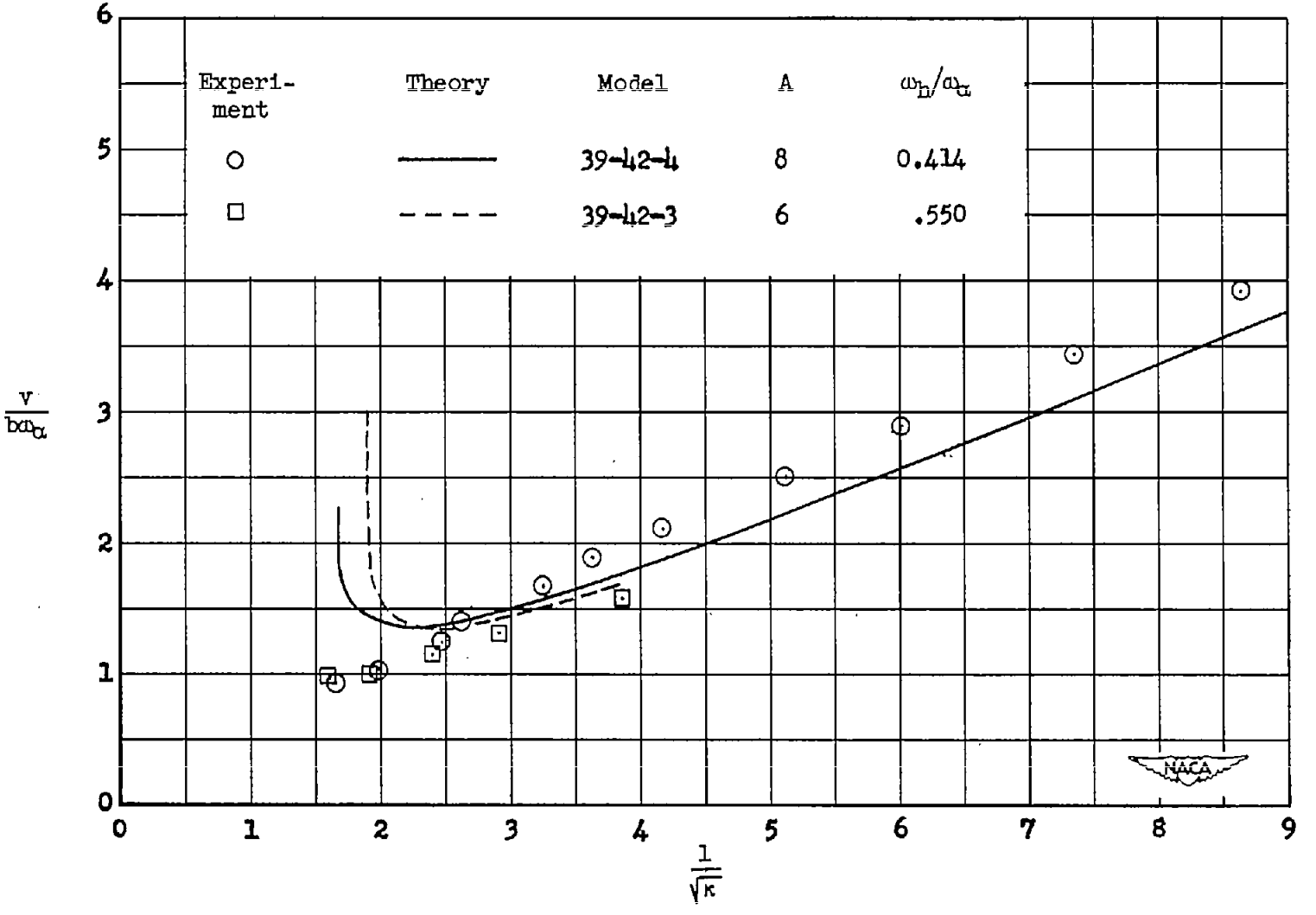

(c) Models 39-42-4 and 39-42-3.

Figure 11.- Concluded.

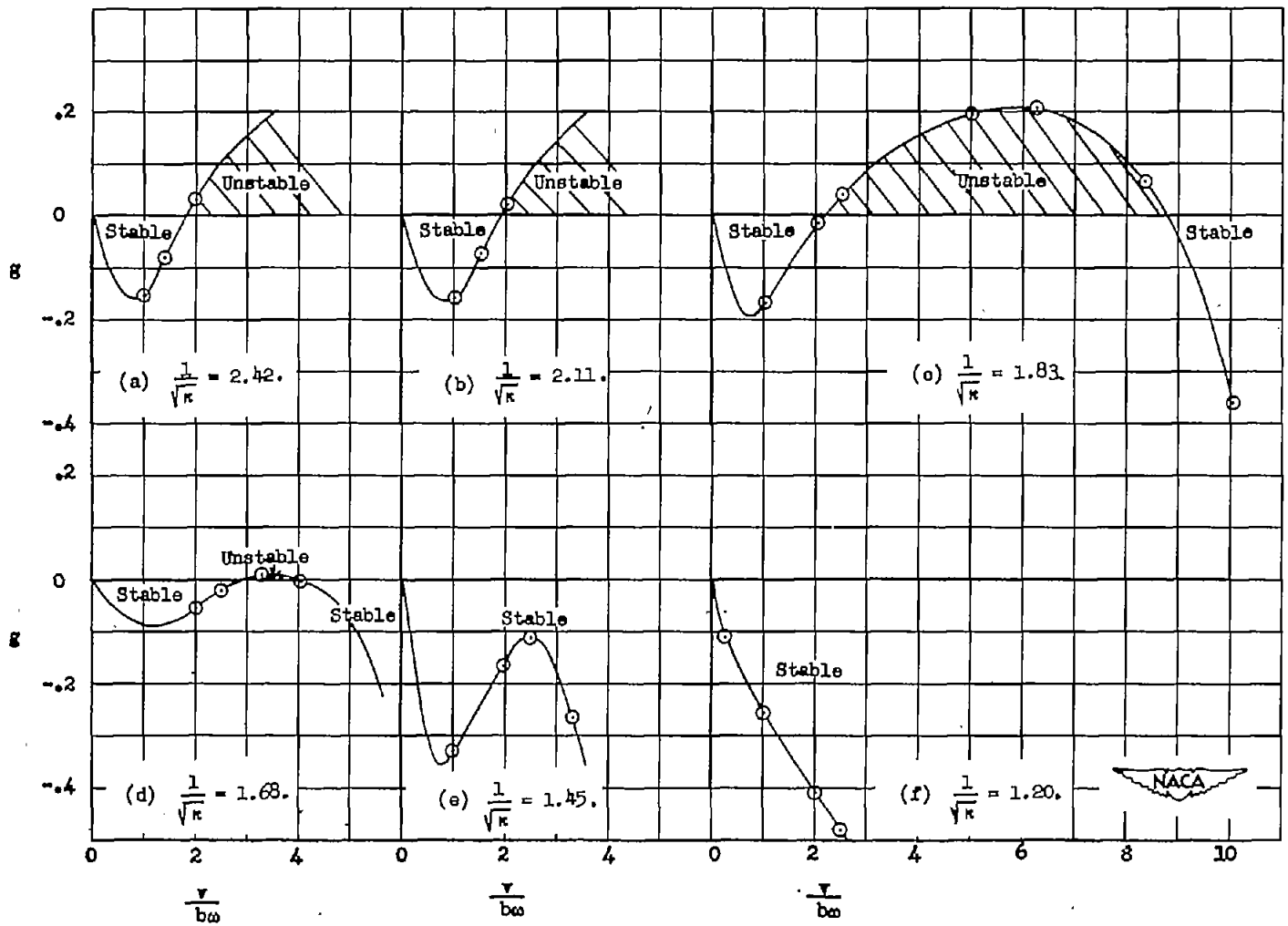

Figure 12.- Plots of damping coefficient g against wave-length parameter $v/b\omega$ from the analytical investigation of model 17-32-3.

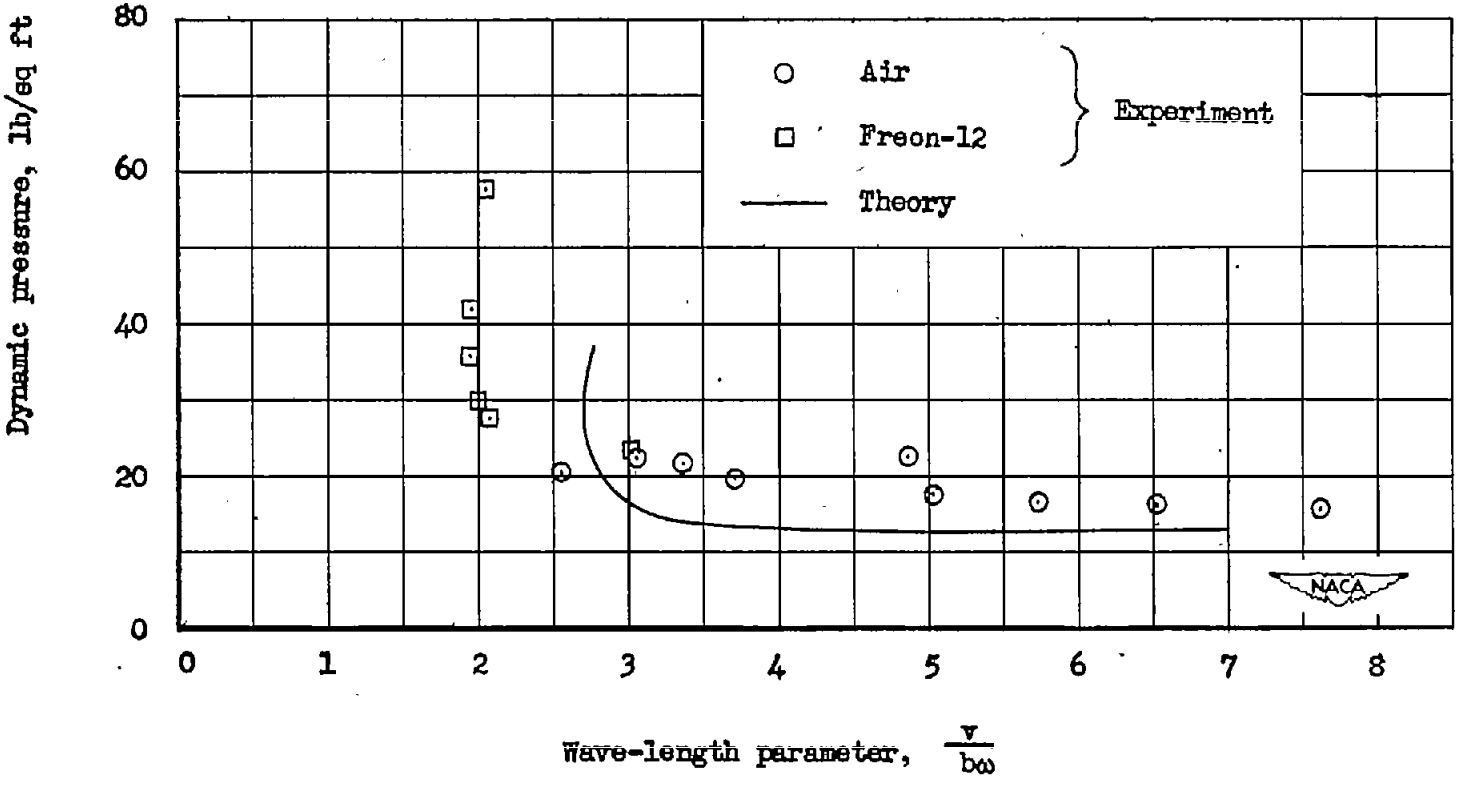

Figure 13.- Dynamic pressure at flutter plotted against wave-length parameter $v/b\omega$ for model 17-32-4.

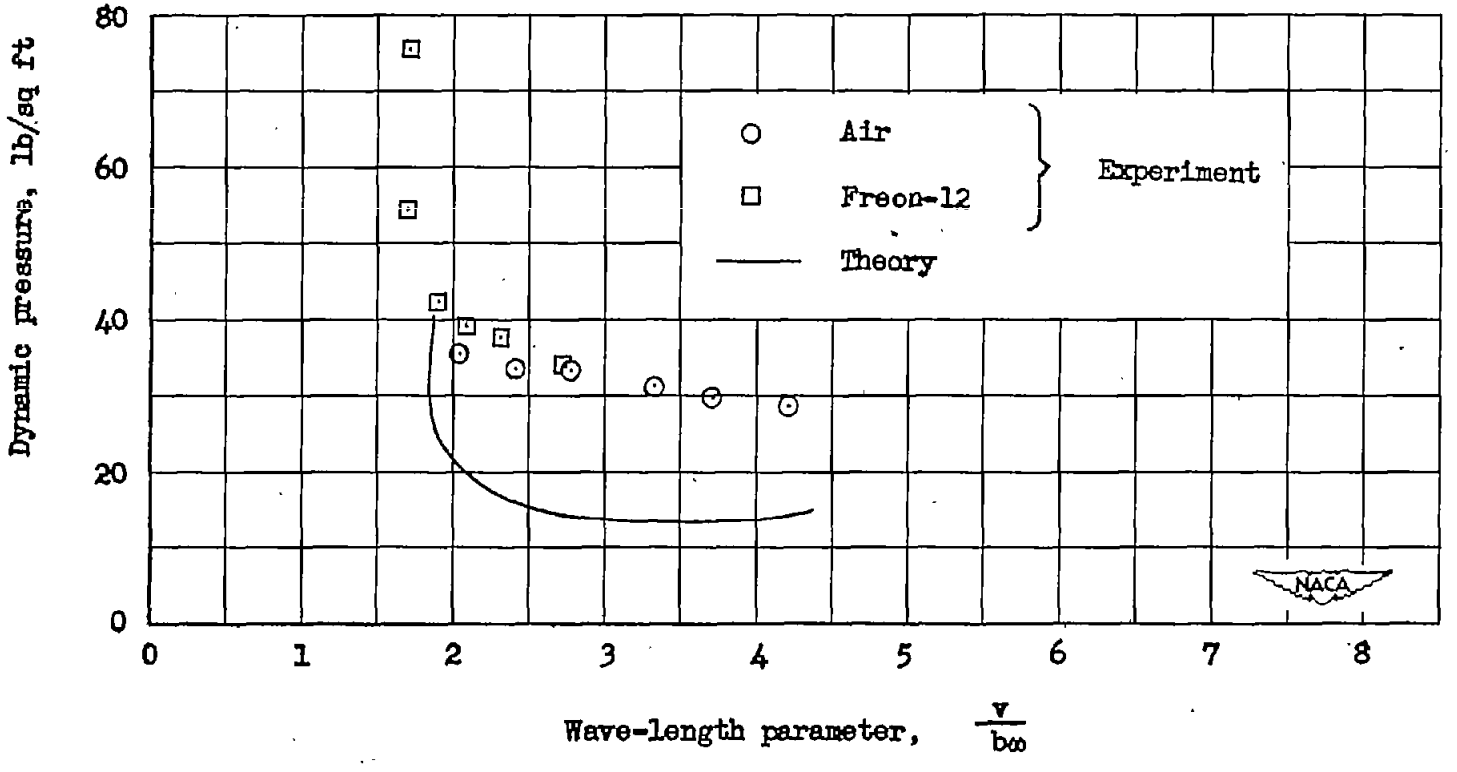

Figure 14.- Dynamic pressure at flutter plotted against wave-length parameter $v/b\omega$ for model 17-32-3.

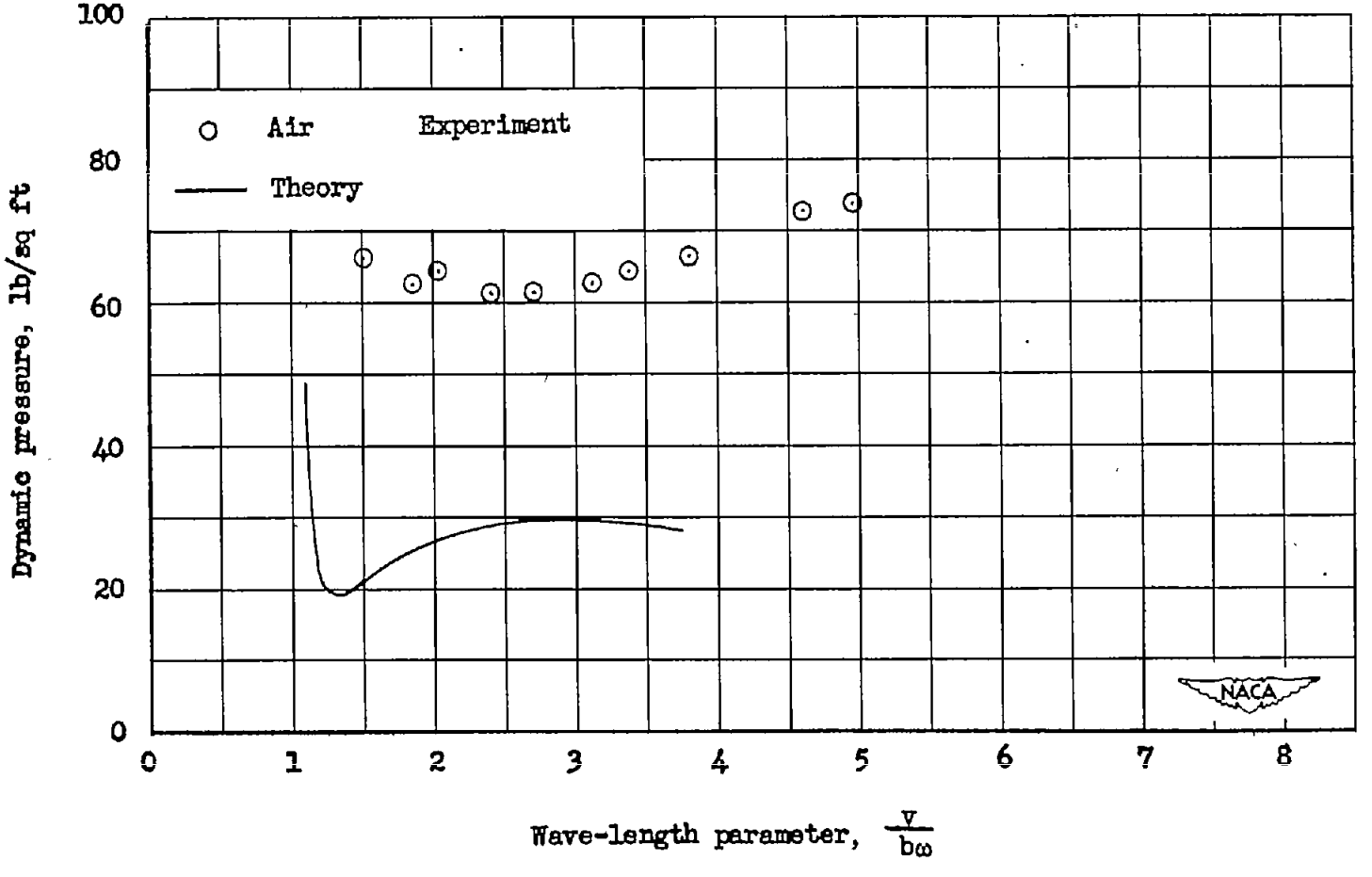

Figure 15.- Dynamic pressure at flutter plotted against wave-length parameter $v/b\omega$ for model 17-32-2.

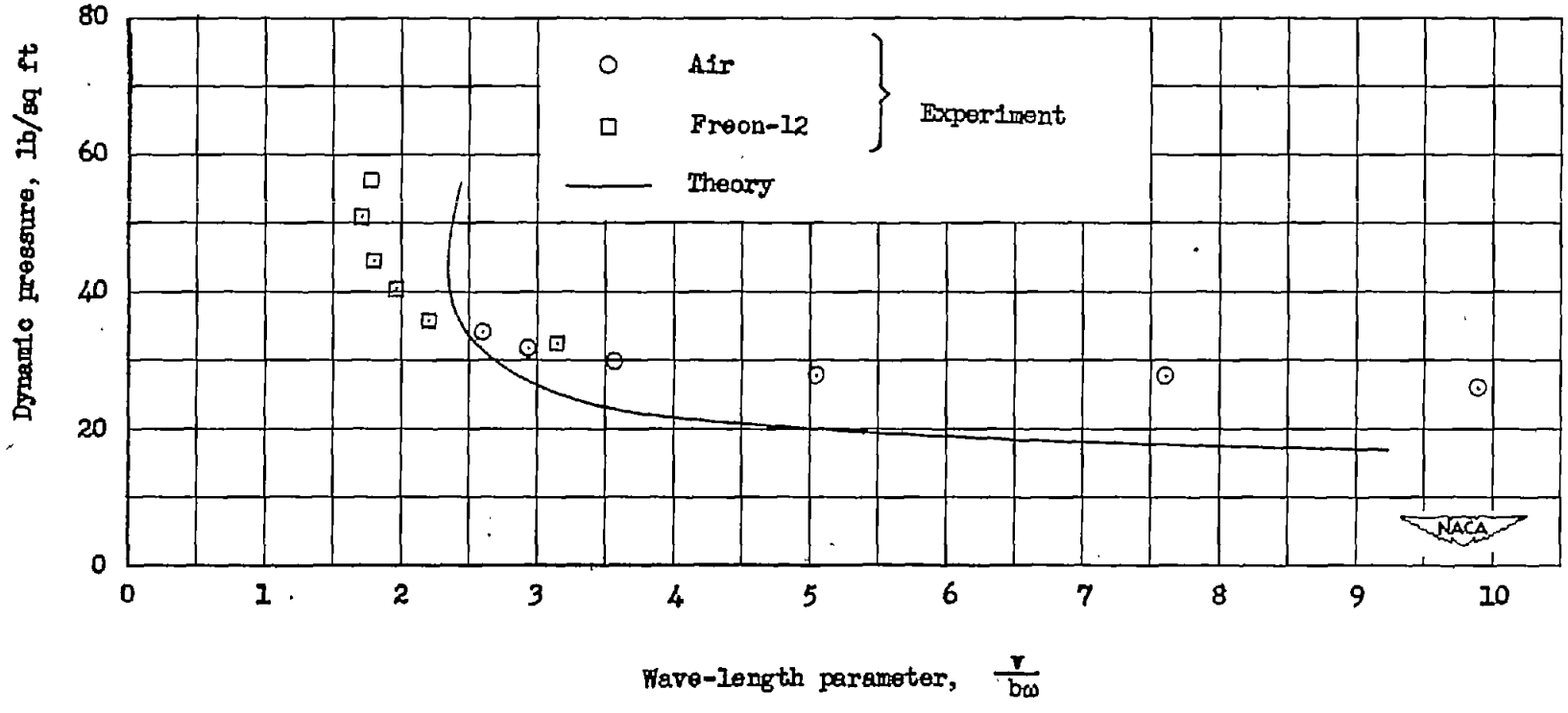

Figure 16.- Dynamic pressure at flutter plotted against wave-length parameter $V/b\omega$ for model 27-38-4.

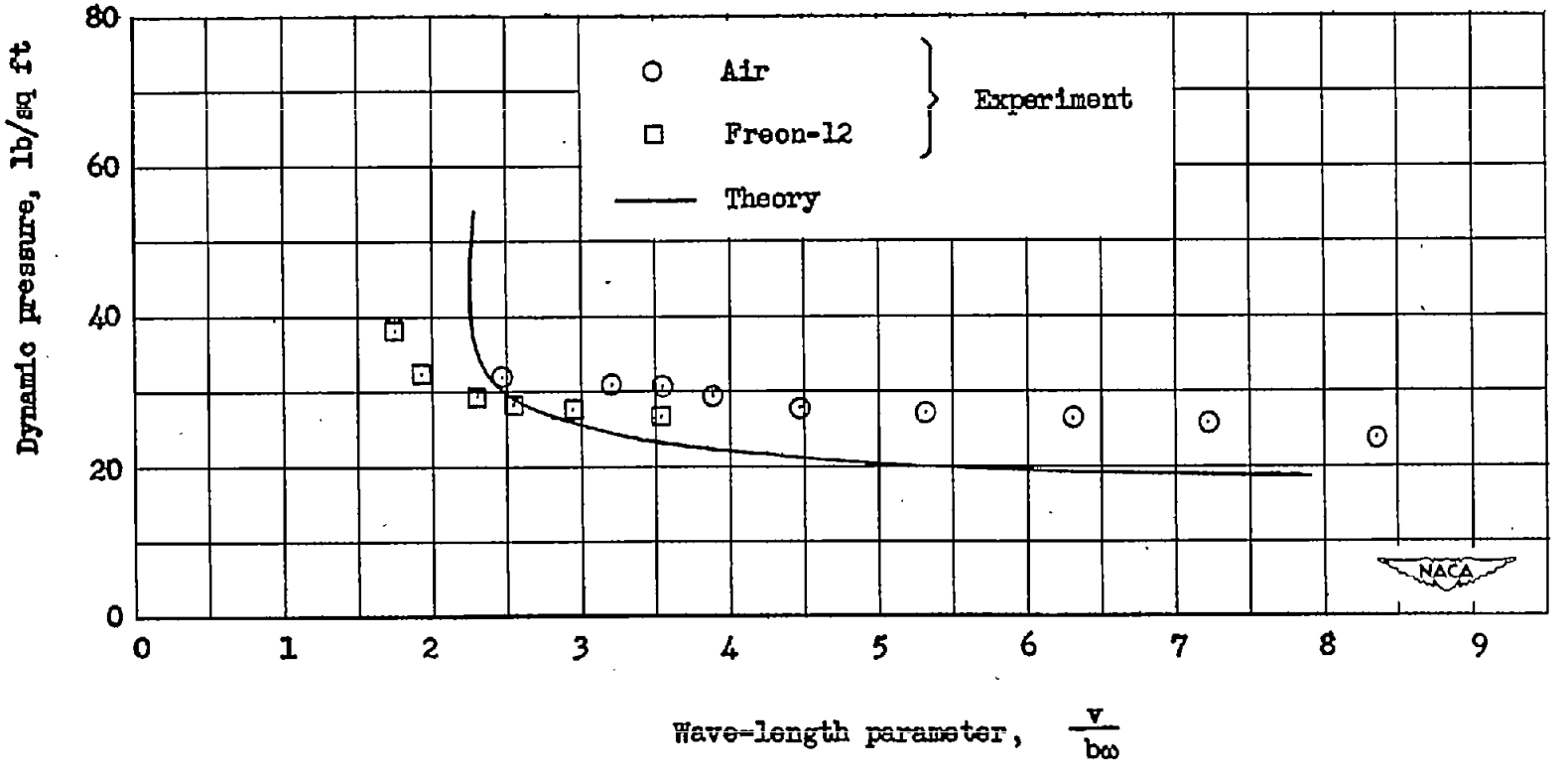

Figure 17.- Dynamic pressure at flutter plotted against wave-length parameter $v/b\omega$ for model 39-42-4.

NACA-Langley - 12-7-51 - 1000